

Current Biology

A Putative Biochemical Engram of Long-Term Memory

Highlights

- Orb2 is required for formation, maintenance, and expression of long-term memory
- Facilitation of Orb2 aggregation lowers the threshold for long-term memory formation
- Extent of Orb2 aggregation correlates with memory strength
- Orb2 aggregation can be used to visualize memory at the molecular level

Authors

Liyang Li, Consuelo Perez Sanchez, Brian D. Slaughter, ..., Jay R. Unruh, Boris Rubinstein, Kausik Si

Correspondence

ksi@stowers.org

In Brief

Si et al. show that aggregates of RNA-binding protein Orb2 could be a potential physical substrate of memory. Inactivation of Orb2 disrupts stable encoding as well as expression of memory, whereas facilitation of Orb2 aggregation allows animals to form memory in suboptimal conditions.

A Putative Biochemical Engram of Long-Term Memory

Liying Li,^{1,2} Consuelo Perez Sanchez,^{1,2} Brian D. Slaughter,¹ Yubai Zhao,¹ Mohammed Repon Khan,¹ Jay R. Unruh,¹ Boris Rubinstein,¹ and Kausik Si^{1,2,3,*}

¹Stowers Institute for Medical Research, 1000 East 50th Street, Kansas City, MO 64110, USA

²Department of Molecular and Integrative Physiology, University of Kansas Medical Center, 3901 Rainbow Boulevard, Kansas City, KS 66160, USA

³Lead Contact

*Correspondence: ksi@stowers.org

<http://dx.doi.org/10.1016/j.cub.2016.09.054>

SUMMARY

How a transient experience creates an enduring yet dynamic memory remains an unresolved issue in studies of memory. Experience-dependent aggregation of the RNA-binding protein CPEB/Orb2 is one of the candidate mechanisms of memory maintenance. Here, using tools that allow rapid and reversible inactivation of Orb2 protein in neurons, we find that Orb2 activity is required for encoding and recall of memory. From a screen, we have identified a DNA-J family chaperone, JJJ2, which facilitates Orb2 aggregation, and ectopic expression of JJJ2 enhances the animal's capacity to form long-term memory. Finally, we have developed tools to visualize training-dependent aggregation of Orb2. We find that aggregated Orb2 in a subset of mushroom body neurons can serve as a “molecular signature” of memory and predict memory strength. Our data indicate that self-sustaining aggregates of Orb2 may serve as a physical substrate of memory and provide a molecular basis for the perduring yet malleable nature of memory.

INTRODUCTION

How a transient experience creates a persistent memory remains a mystery. A long-standing conceptual framework of memory is the idea of an “engram”: experience produces an enduring physical substrate or “engram” in the nervous system [1], which allows memory to persist over time, and activation of the engram allows recall of the past experiences [2, 3]. Among others, Wilder Penfield [4] divided the memory engram into two basic components, molecular—“(1) what are the basic protoplasmic alterations that make permanent recording of experience and memory recall possible?”—and cellular/network based—“(2) how and where does the neurone transaction take place that constitutes the record of experience and makes possible its reproduction or recall?” Discovery of activity-dependent change in synaptic activity and network properties [5, 6] provided a cellular basis to the engram idea. Imaging of activated neurons and manipulation of neuronal activity in *Drosophila* [7, 8] and in mice [9–13] has led to the identification of sets of neurons or engram cells that are recruited when memories are formed, and activation of these neurons is necessary and sufficient to retrieve a memory.

However, the biochemical changes in the engram cells that allow storage and recall of memory remain unclear.

Protein synthesis in neurons has been linked to long-term change in synaptic efficacy and long-term memory [14, 15], particularly for consolidation and persistence of new memories and reconsolidation of existing memories [16]. Among various regulators of protein synthesis, cytoplasmic polyadenylation element-binding proteins (CPEBs), a family of RNA-binding proteins, is of particular interest [15]. Some CPEB family members, including *Aplysia* CPEB, *Drosophila* Orb2, and mouse CPEB3, possess the ability to exist in two states: a monomeric state and a self-sustaining amyloidogenic aggregated state akin to prion-like proteins [17–20]. More importantly, the aggregated state is necessary for the persistent change in synaptic activity in *Aplysia* [21–23] and persistence of memory beyond 1 day in *Drosophila* [24–26] and in mouse [27]. The Orb2 gene has two distinct protein isoforms: Orb2A and Orb2B (Figure 1A) [26, 28, 29]. The Orb2B protein is abundant and constitutive, whereas Orb2A is extremely rare and sparsely expressed. In spite of its low abundance, the Orb2A isoform acts as a seed to induce oligomerization of Orb2B, and Orb2A-dependent oligomerization is required for the persistence of memory [25, 26, 30]. In *Drosophila*, conversion to the aggregated state transforms Orb2 from a translation repressor to an activator [31] and regulates translation of genes that are important for synaptic growth and synaptic activity [32].

Taken together, these observations suggest a model in which CPEB proteins act as a bi-stable switch. Experience converts it from a monomer into a self-sustaining aggregated state and creates an enduring biochemical alteration in specific neurons (and synapses) and maintains memory over time. This model raises the following fundamental yet unanswered questions: (1) When and how long is Orb2 activity required once a stable memory is formed? (2) What aspects of memory are dependent on Orb2: storage, recall, or both? (3) What are the consequences, if any, of artificially enhancing aggregation of Orb2? (4) Where does Orb2 aggregation occur, and can aggregated status of Orb2 inform about the strength of memory? Here, we have addressed these questions.

RESULTS

A System for Rapid and Reversible Inactivation of *Drosophila* Orb2 Protein

Determination of the requirement of Orb2 in various phases of memory requires a method to transiently inactivate the Orb2

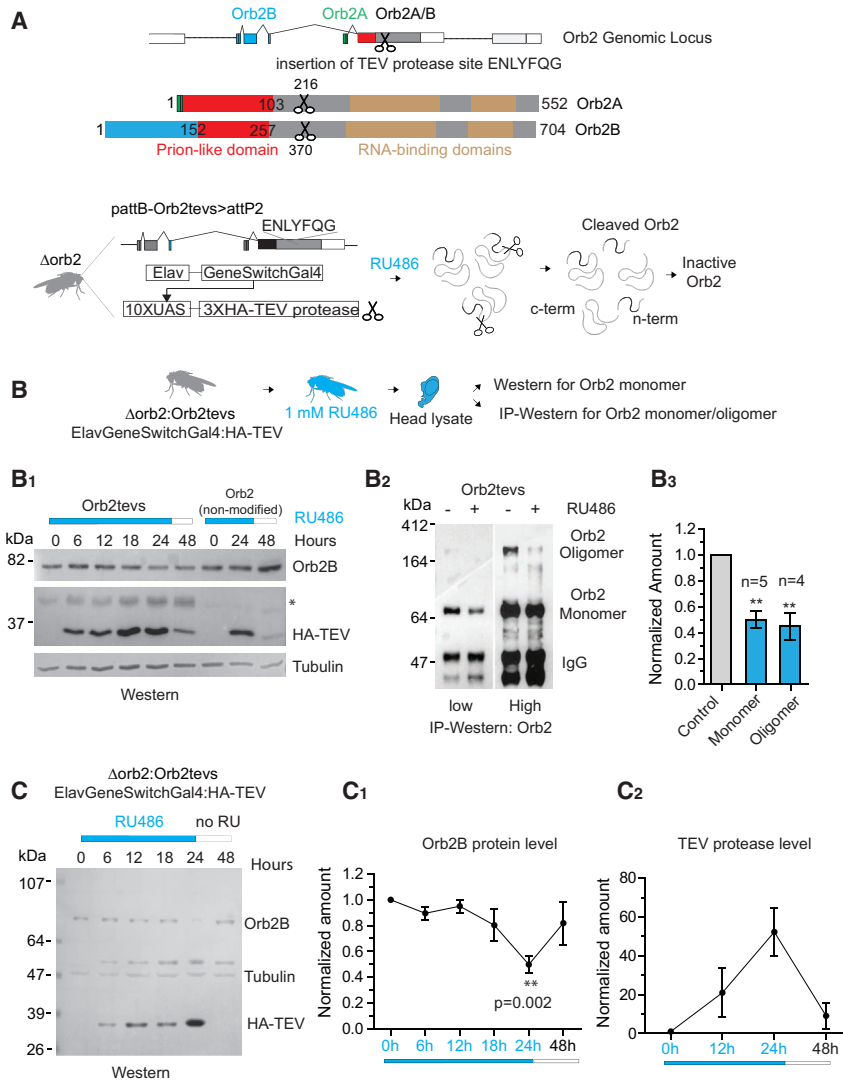


Figure 1. A System to Acutely and Reversibly Inactivate *Drosophila* Orb2 Protein

(A) Position of TEV protease recognition site (tevs) insertion in Orb2 proteins and schematic of the experimental design. An Orb2 genomic fragment bearing a TEV protease recognition sequence (tevs) ENLYFQG was introduced in *orb2*-null flies, and expression of HA-tagged TEV protease was induced in neurons by RU486 to cleave and inactivate Orb2tevs protein.

(B) Orb2tevs monomer and oligomers are cleaved by TEV protease in vivo. (B₁) Orb2tevs and non-modified Orb2 flies were fed with RU486 (blue bar) to induce TEV protease expression and then retrieved from RU486 (white bar) to reduce TEV protease expression. Samples were collected at indicated time point and western blotted for monomeric Orb2 and HA-TEV. (B₂) Orb2tevs flies were fed RU486 for 24 hr and subjected to immunoprecipitation (IP)-western. Two different exposures of the same gel are shown to illustrate the reduction in both monomer (low) and oligomer (high) level. (B₃) Quantification of monomer and oligomer level after 24 hr of RU486 feeding normalized to vehicle control is shown.

(C) Recovery of monomeric Orb2 level following removal of RU486. (C₁) Quantification of total monomeric Orb2 protein and (C₂) TEV-protease following 24 hr 1 mM RU486 feeding (blue) and 24 hr after withdrawal of RU486 (black) is shown. The protein levels were normalized to 0-hr time point. The data are expressed as mean \pm SEM, and statistical significance was determined by using one-way ANOVA (Tukey multiple comparison) for more than two samples or unpaired t test for two samples. ** $p \leq 0.01$ and *** $p \leq 0.001$. See also Figure S1.

1 mM RU486 within 4–6 hr induced HA-TEV protease and resulted in a gradual decrease of Orb2 protein (Figures 1B and 1B₁). After 24 hr, there was an ~50% reduction in both forms of Orb2

protein in the nervous system. Gene deletion or RNAi were not useful for this purpose because (1) they create a chronic depletion of the protein and (2) rely on normal decay of the existing proteins, whereas aggregates of Orb2 are stable [28], requiring inactivation of the existing protein not just elimination of new Orb2. To this end, we have developed a conditional Orb2 protein inactivation system by inserting the tobacco etch virus (TEV) protease [33] recognition sequence ENLYFQG (tevs) at various sites within the Orb2 protein (Figure S1A) and introducing a genomic fragment bearing the modified Orb2 (Orb2tevs) in an *orb2*-null background. One of these positions in the common exon of Orb2A/Orb2B (amino acid [aa] 370 for Orb2B and aa 216 for Orb2A; Figure 1A) produces a Orb2tevs protein that is functionally equivalent to wild-type Orb2 [31] and rescues all *orb2* deficiencies, and TEV protease cleaves and renders both monomeric and oligomeric Orb2tevs translationally inactive [17, 31]. To determine whether this system could reversibly deplete Orb2, we used a RU486 inducible neuron-specific ElavGeneSwitch-Gal4 driver [34, 35] to express hemagglutinin (HA)-tagged TEV protease (Figure 1A). Feeding of

(0.50 \pm 0.06 in monomer and 0.45 \pm 0.10 in oligomer; Figures 1B, 1B₂, and 1B₃). Upon removal of the RU486, the TEV protease level dropped significantly (0.79 \pm 0.07; $n = 4$) within 24 hr (Figures 1C and 1C₂) with a corresponding increase in monomeric Orb2 protein level almost to the wild-type level (0.82 \pm 0.17; Figures 1C and 1C₁). The relatively rapid disappearance of TEV protease upon RU486 withdrawal is most likely due to the limited period of RU486 exposure and short half-life of TEV protease. Taken together, these results suggested the Orb2tevs-TEV system can be used to transiently reduce the Orb2 protein level from adult neurons.

Orb2 Activity Is Required for Encoding and Retrieval of Long-Term Memory

To determine the behavioral consequence, if any, of transient depletion of Orb2 protein, we exposed flies to 1 mM RU486 or to vehicle only as a control and assessed long-term memory in the male courtship suppression paradigm (Figure 2A). In this paradigm, a male fly learns to suppress its courtship behavior for days after repeated rejection by an unreceptive female

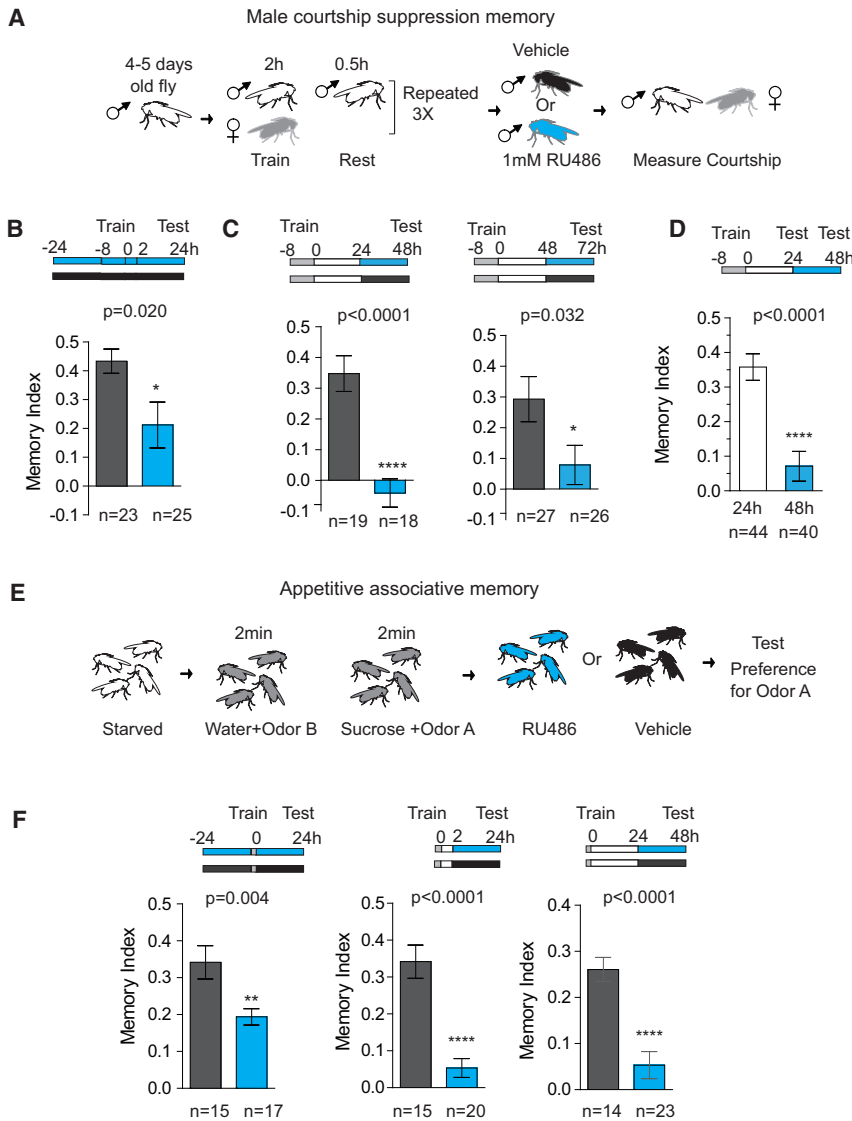


Figure 2. Orb2 Activity Is Required to Maintain Memory Days after Its Formation

(A) Schematic of the male courtship suppression memory paradigm. Virgin males were isolated for 4 or 5 days prior to training and then exposed to a freshly mated female. Flies were either fed with 1 mM RU486 (blue) or vehicle (black) before testing with another mated female.

(B) Feeding of RU486 before, during, and immediately after training reduces memory.

(C) Feeding of RU486 any time after training reduces memory. Schematic of RU486/vehicle feeding at different time period post-courtship suppression training (top) and the memory index after 24 hr of feeding (bottom) are shown.

(D) RU486 feeding reduces existing memory. The same sets of flies were tested before (24 hr) and after feeding (48 hr).

(E) Schematic of the appetitive associative memory paradigm. 1- to 2-day-old flies were starved for 18–22 hr and then trained to associate either MCH or OCT with 1 M sucrose as reward. Following training, flies were given either 1 mM RU486 (blue) or vehicle (black) and then starved again before testing for their odor preference.

(F) Feeding of RU486 before and any time after training reduces appetitive-associative memory. Memory index for each group was plotted as mean ± SEM, and statistical significance was determined by unpaired t test.

*p < 0.05, **p < 0.01, and ***p < 0.001. See also Figure S1.

[36, 37]. Compared to vehicle controls, flies fed with RU486 before, during, and immediately after training had significantly less memory after 1 day (Figure 2B), consistent with previous studies [24, 26, 38]. Feeding of RU486 to genetic controls had no effect on long-term memory (Figure S1B).

To determine the temporal requirement of Orb2 after formation of memory, we gave flies either RU486 or vehicle immediately after (Figure S1B), 1 day after, or 2 days after training and tested memory at the end of 24 hr of RU486 feeding (Figure 2C). Compared to the vehicle, feeding of RU486 at any time after training resulted in a significant reduction ($p < 0.05$) in memory score after 1 day (Figures 2C and S1B). To distinguish between the possibilities that (1) the RU486-fed flies have never formed any memory and (2) they have formed memory but failed to maintain and/or retrieve it, we tested a group of flies 24 hr after training to ensure memory formation, exposed them to RU486 for 24 hr, and then tested them a second time. Exposure to RU486 resulted in a significant reduction in already-formed memories (Figure 2D). To test whether such

Similar to the courtship suppression paradigm, flies fed with RU486 before or immediately after training or 1 or 2 days post-training resulted in a significant loss in memory within the subsequent 24 hr (Figure 2F). Feeding of RU486 did not interfere with memory of flies expressing only TEV protease or Orb2tevS (Figure S1C). Taken together, these results suggest Orb2 activity is required days after memory formation in at least two distinct memories.

The loss of already-formed memory could be due to an inability to retrieve/express the stored memory and/or impairment in memory storage. If Orb2 is only involved in retrieval, depletion of Orb2 during memory formation and restoration of Orb2 during recall should be sufficient for memory to express. When flies were fed with RU486 before and during training and then removed for 1 or 2 days to re-express Orb2 before testing (Figures 3A and S1D), there was no memory, suggesting that Orb2 is required to establish a memory. We wondered what would happen if Orb2 is restored following disruption of an already-established memory. To this end, flies were trained

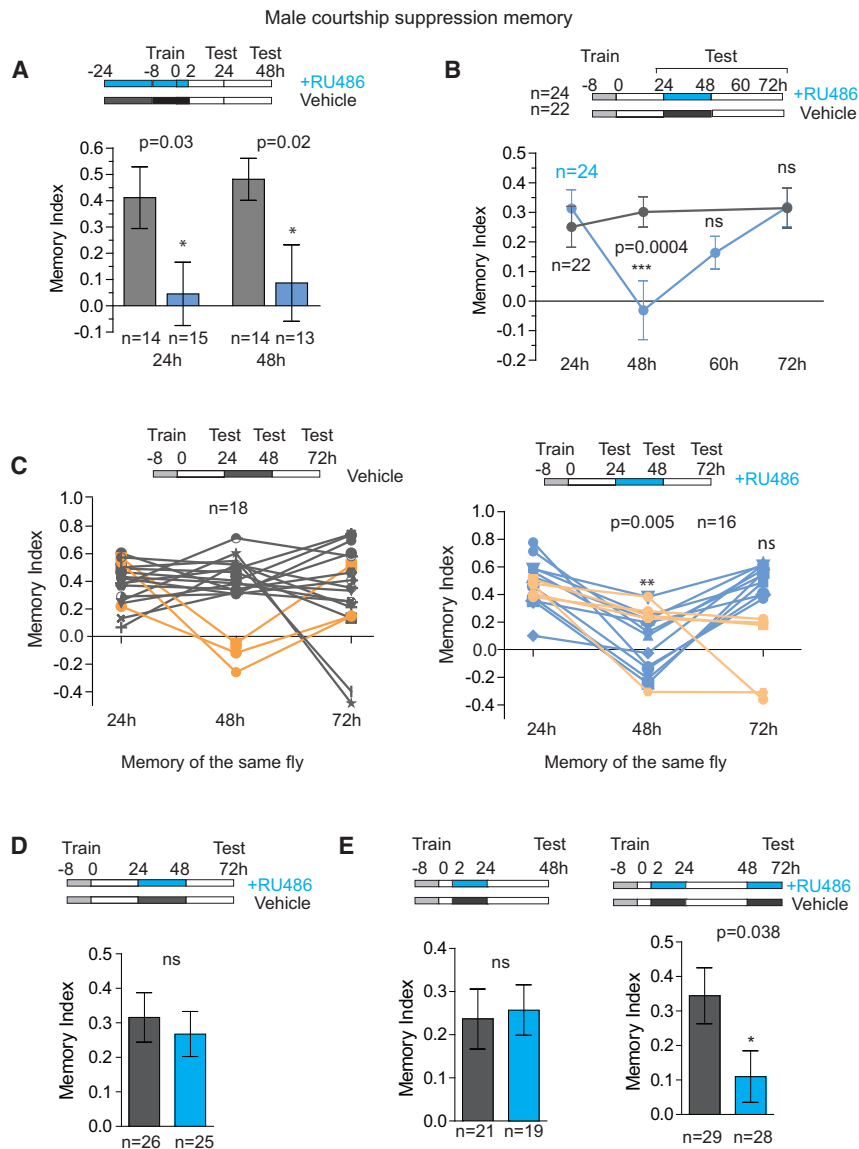


Figure 3. *Orb2* Is Required for Storage, Retrieval, and Recovery of Memory in the Courtship Suppression Paradigm

(A) Reducing *Orb2* during or immediately after training and providing only during recall is not sufficient for courtship-suppression memory. Flies were fed with RU486 (blue) or vehicle (black) 24 hr before, during, and 2 hr after training and then back to normal food for 24 hr or 48 hr before testing.

(B) Once established, memory can recover if *Orb2* is re-expressed. One day after training, flies were fed with RU486 or vehicle for 24 hr and then transferred back to normal food for 12 hr (60 hr) or 24 hr (72 hr) before testing. The same group of flies were trained and tested at 24 hr, 48 hr, 60 hr, and 72 hr post-training.

(C) Memory recovery in the same fly. Memory score of the same individual fly at 24 hr, 48 hr, and 72 hr. One day post-training, flies were fed with vehicle (left) or RU486 (right). Feeding of RU486 or vehicle was restricted between 24- and 48-hr periods. Each line represents memory dynamics of individual fly at indicated time point. Black (vehicle) and blue (RU486) lines represent the main trend, and orange lines represent deviations from the main trend. (B) and (C) are independent experiments.

(D) Memory recovery is independent of testing. Flies trained in the male courtship suppression paradigm were fed RU486 (blue) or vehicle (black) for 24 hr 1 day after training and then back to normal food for 24 hr before testing (white).

(E) Recovered memory requires *Orb2*. Flies were fed with RU486 (blue) or vehicle (black) during two indicated periods of time: 2–24 hr (left) and 48–72 hr (right) and memory was tested at 48 hr (left) and 72 hr (right). The flies were rested for 2 hr before RU486 exposure to allow memory formation. Memory index at each time point was plotted as mean \pm SEM.

See also Figure S1.

and 24 hr after training exposed to RU486 for 1 day and then removed from RU486; memory was tested after 12 hr and 24 hr. Unlike the vehicle-treated group that maintained their memories in all time points tested, for flies that formed memories 24 hr after training, their memory was reduced upon exposure to RU486 as expected; however, surprisingly, memory gradually recovered upon withdrawal of RU486 (Figure 3B). To verify that memory indeed changed in the same fly, in an independent set of experiments, we plotted the memory score of each individual fly at three time points after training: before exposure to RU486; 24 hr after RU486 treatment; and 24 hr after withdrawal of RU486 (Figure 3C), and we observed a similar loss and recovery of memory in individual flies. The memory recovery is not a consequence of multiple testing (which may reinforce memory), because testing only once at the end showed similar recovery as multiple testing (Figure 3D). Similarly, recovery is not because memory has become independent of *Orb2*, because following memory recovery (Figure 3E, left), inactivating *Orb2* again before

testing resulted in memory impairment (Figure 3E, right). These observations suggest that *Orb2* is required for formation/en-

JJJ2, an Hsp40 Chaperone, Enhances *Orb2A* Aggregation

coding as well as retrieval of memory, and reduction of *Orb2* after memory establishment results in transient amnesia.

Mutations in *Orb2* or peptide inhibitors that prevent *Orb2* aggregation suggested that the conformational switch of *Orb2* to the aggregated state is important for long-term memory [24–26, 30, 38, 41]. However, the consequence of facilitation of *Orb2* aggregation, if any, is still unknown. Chaperones are proteins that guide protein folding and maintain protein homeostasis [42]. Previously, we found that the *Orb2A* prion-like domain (*Orb2AprD*) can substitute the yeast Sup35 prion-like domain and that the *Orb2AprD*-Sup35C fusion protein readily undergoes prion-like conversion in yeast [17]. Others have reported that yeast chaperones, such as Hsp104, can influence aggregation of mammalian proteins [43, 44]. Therefore, we carried out an unbiased survey of the chaperones in yeast *S. cerevisiae* [45] by

knocking out 38 nonessential chaperones in a background that allows for the score of prion-like conversion of an Orb2AprD-Sup35C chimeric protein (Figures 4A and S2). In a reciprocal screen, we overexpressed 57 out of 63 individual yeast chaperones by a galactose-inducible system (Figures 4B and S3). Both the deletion and overexpression screen consistently identified JJJ2, a lowly expressed (~200 molecules/cell; Yeast Genome Database) DNA-J-domain-containing protein in Hsp40 family [45, 46] that surprisingly facilitates the aggregation of Orb2AprD-Sup35C protein. When Orb2AprD-Sup35C is in the aggregated (prion-like) state, cells are white and can grow in media lacking adenine and in non-aggregated state cells are red and cannot grow in media lacking adenine. In the absence of JJJ2, Orb2AprD-Sup35C primarily exists in the red-Ade state (Figures 4A and S2C), whereas upon overexpression, cells adopt the white +Ade state in higher frequency (Figure 4B). Interestingly, deletion of JJJ2 had no significant effect on the prion-like conversion of Orb2BprD-Sup35C, yeast prions RNQ1-Sup35C, or MOT3-Sup35C (Figure S2D) fusion proteins. Hsp40, a family of chaperones (~23 in yeast and ~43 in *Drosophila*) stimulate the ATPase activity of Hsp70 and deliver specific client proteins to Hsp70 [47]. Recent studies found different yeast prions utilize specific Hsp40 family members [48, 49], suggesting that JJJ2 may target a limited number of proteins and may modify Orb2 aggregation.

JJJ2 Enhances Orb2 Aggregation in Heterologous System

To test whether JJJ2 as a yeast protein could be used as a tool to influence Orb2 aggregation in *Drosophila*, we co-expressed JJJ2 with Orb2A or Orb2B in S2 cells. To our surprise, in the presence of JJJ2, the monomeric Orb2A protein migrated in a position higher than Orb2A alone and the SDS-resistant aggregates of both Orb2A and Orb2B were increased (Figure 4C). Expression of just the N-terminal 66 amino acids of JJJ2 encompassing the DNA-J domain (J-only) or JJJ2 lacking the 66 amino acids (JJJ2ΔJ) was less effective in inducing aggregation (Figures 4C and S4A). Interestingly, only a fraction of JJJ2 copurifies with Orb2 proteins (Figure S4B) and Orb2A-JJJ2 aggregates partially overlap. We also find JJJ2 enhances but does not alter the dynamics of Orb2A aggregates based on fluorescence recovery after photobleaching (FRAP) studies (Figures S4C and S4D).

Are these JJJ2-induced Orb2 aggregations functionally relevant? Previously, using an in vitro Orb2-dependent translation system, we have observed that monomeric Orb2 reduces, whereas aggregated Orb2 enhances, translation [31]. In the in vitro translation system, addition of the N-terminal 320aa of Orb2A, encompassing the prion-like domain, induced aggregation of Orb2B and enhanced translation, as we have found previously (Figure 4D). Addition of JJJ2 alone also resulted in an increase in Orb2-dependent translation, whereas addition of both Orb2A-320 and JJJ2 resulted in a further increase in translation (Figure 4D). This JJJ2-mediated increase requires Orb2-protein and full-length JJJ2: addition of JJJ2 in *orb2*-null extract (Figure 4D, right) or in strong hypomorphic Orb2Δ80Q extract (Figure S4E) or addition of JJJ2ΔJ or just J-domain in wild-type extract (Figure 4D, left) had no activating effect. Likewise, a translation reporter with a mutation in its Orb2-binding site

(M2P) was also unaffected by the addition of JJJ2 (Figure S4F). Taken together, these results suggest that JJJ2 not only affects Orb2 conformation, it also affects Orb2-mediated translation.

Expression of JJJ2 Enhances Memory

Next, we sought to determine whether JJJ2 influences long-term memory and generated transgenic flies expressing HA-tagged JJJ2 under the Gal4-upstream activating sequence (UAS) system [50]. Flies carrying JJJ2 as a transgene were similar to wild-type flies in fecundity, lifespan, locomotion, and sensory perception. Normally, in the male courtship suppression memory paradigm, three 2-hr training sessions (Figure 2A) are required to generate long-term memory; one training session of 2 hr leads to no or low memory in wild-type flies (Figure 5A) [26, 36]. Unexpectedly, we observed that flies harboring a single copy of JJJ2 transgene (UAS-JJJ2-HA>attp40), even in the absence of any Gal4 driver, formed significantly higher memory following one (Figure 5A) or two training sessions (Figure S5A), and the memory persisted over days. Immunopurification revealed low level of JJJ2HA protein expression in the UAS-JJJ2HA>attp40 adult fly head (Figure S5B). The following controls suggest memory enhancement is not an artifact of insertion at attp40 site in the second chromosome and requires full-length JJJ2 protein expression (Figure 5B): there was no increase in memory in flies harboring (1) JJJ2 with a single nucleotide frameshift after the fifth amino acids that introduces a stop codon in all three reading frames (UAS-JJJ2FS>attp40); (2) JJJ2 lacking the DNA-J domain (UAS-JJJ2ΔJ>attp40) [51]; (3) only the 66-amino-acid DNA-J domain (UAS-J domain>attp40); (4) the close family member JJJ3 (UAS-JJJ3HA>attp40); or (5) full-length wild-type JJJ2 at attp2 site on the third chromosome (UAS-JJJ2HA>attp2) that did not show any detectable expression (Figures S5B and S5C). The UAS-JJJ2>attp40 also failed to improve memory of Orb2Δ80Q flies lacking the part of the prion-like domain [24], indicating that JJJ2-mediated memory improvement either requires Orb2 or cannot circumvent the Orb2 deficiency (Figure 5B). Finally, to determine the effect of Gal4-driven expression, UAS-JJJ2>attp40 flies were crossed to 201Y-Gal4 to drive expression in the mushroom body. Crossing to 201Y resulted in an increase in memory following 1× training only in JJJ2, but not in controls (Figure S5D).

To test the generality of memory-enhancing phenotype of JJJ2, we also tested the flies in the associative appetitive memory paradigm (Figure 2E), in which the nature of the sugar determines the strength of memory. For example, a sweet nutritious sugar, such as sucrose, produces both short- and long-term memory, whereas sweet but non-nutritious sugars L-sorbose, D-xylose, or D-arabinose produce short-term but low long-term memory and non-sweet but nutritious sorbitol does not produce any memory [52]. Expectedly, wild-type flies had very low memory of L-sorbose, D-xylose, or D-arabinose at 24 hr (Figure 5C). In contrast, UAS-JJJ2HA>attp40 flies form significantly higher memory ($p < 0.05$) with all three sugars compared to wild-type flies (Figure 5C). We even observed significantly higher 24-hr memory in UAS-JJJ2>attp40 group with sucrose (Figure 5D) and fructose (Figure S5E) with concentration reduced to 100 mM. JJJ2 lacking the J domain or carrying only the J domain or JJJ2 in the Δ80QOrb2 background had no effect on appetitive-associative memory either (Figure 5D), and crossing

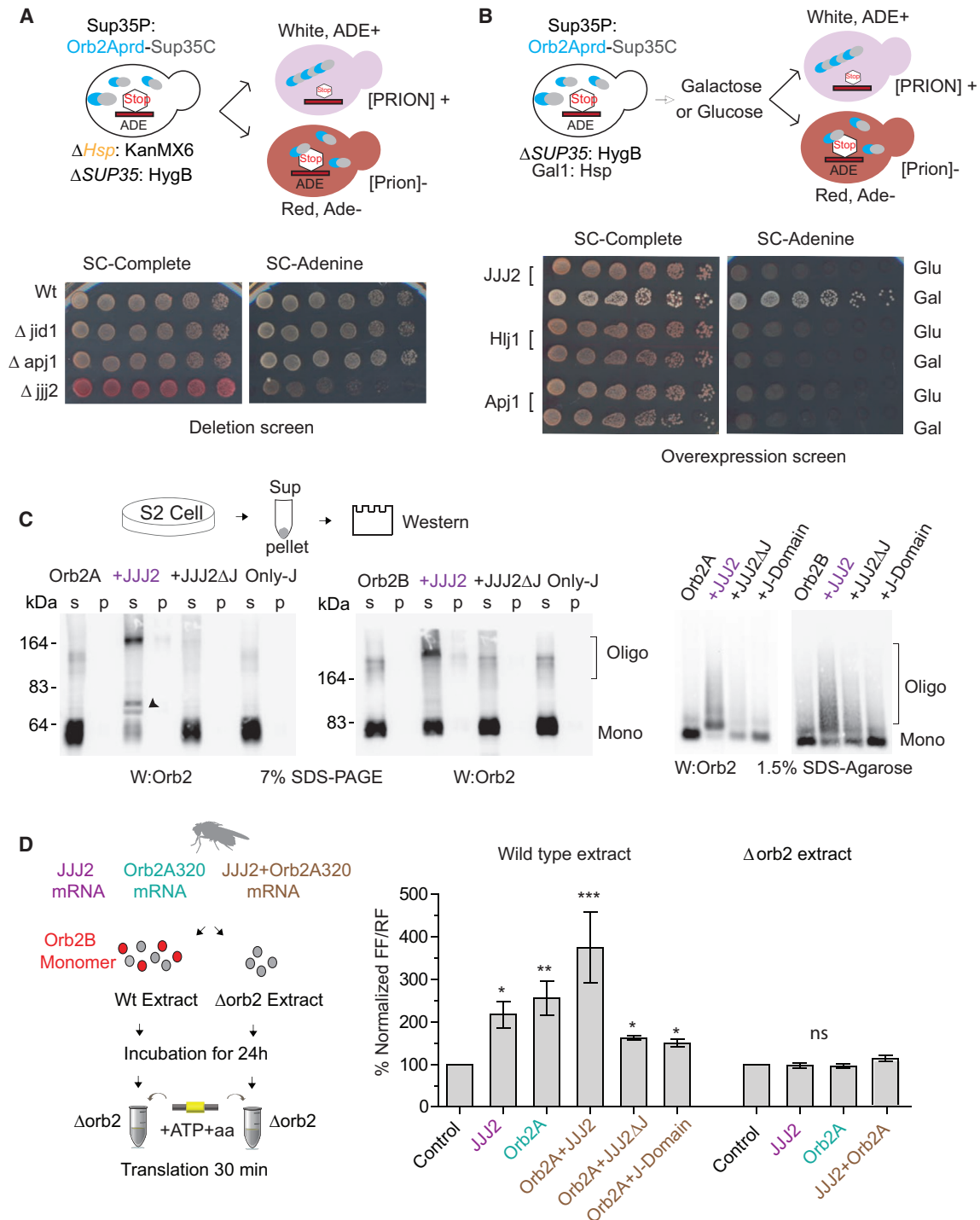


Figure 4. Yeast Hsp40 Family Protein JJJ2 Enhances Functional Orb2 Aggregates in Heterologous System

(A) Top: schematic of yeast Hsp deletion screen. Bottom: in JJJ2 deletion background, but not in wild-type or other Hsp40s, such as Jid1, or Apj1 deletion background, colonies appear red in rich media and grow slowly on –adenine media.

(B) Top: schematic of yeast Hsp overexpression screen. The chaperones were ectopically expressed under the inducible Gal promoter in Orb2Aprd-Sup35C background. Same strains grown in glucose serve as a control. Bottom: overexpression of JJJ2, but not other Hsps, such as Hlj1 or Apj1, facilitates growth in –adenine media.

(C) JJJ2 induces aggregation of Orb2A and Orb2B in S2 cells. The cell lysate was run in 7% SDS-PAGE (left) or 1.5% SDS-agarose gel (right) to reveal monomeric and oligomeric Orb2. JJJ2 Δ J (JJJ2 protein lacking the N-terminal 66 amino acids encompassing the DNA-J domain) and only-J (N-terminal 66 amino acids of JJJ2 containing the DNA-J domain) serve as control. S and P indicate supernatant and pellet, respectively.

(legend continued on next page)

to 201YGal4 resulted in memory increase only in JJJ2, but not in the control (Figure S5F). Similar to courtship, suppression memory insertion of UAS-JJJ2 at the third chromosome attP2 site did not improve memory (Figure S5G). However, when crossed to mushroom body Gal4 driver (201YGal4: UAS-JJJ2>attP2), it enhanced memory (Figure S5G).

Intriguingly, JJJ2 had no measurable effect on training conditions that generate robust long-term memory, such as 3× training in courtship conditioning (Figure S5A) or 1 M sucrose in appetitive conditioning (Figure 5E), or training conditions that do not produce any long-term memory, such as 10 mM sucrose or 1 M sorbitol in the appetitive memory paradigm (Figure 5E). Moreover, starvation is required for long-term appetitive memory [53]; when non-starved UAS-JJJ2>attP2 flies were trained with D-arabinose, they failed to produce long-term memory (Figure 5F). Finally, in the heat-box operant conditioning, which generates short-term memory [54], JJJ2 had no effect (Figure S5H), suggesting that JJJ2 has not created a state that in general improves all sensory processing or associations. Therefore, very low levels of JJJ2 lower the threshold for long-term memory formation but cannot de novo produce long-term memory or override all restrictions to long-term memory formation. It is unclear whether JJJ2 phenotype is solely mediated through Orb2.

Reconstitution of TEV Protease Activity in Orb2-Aggregation-Dependent Manner

Because Orb2 is required to encode and retrieve long-term memory and facilitation of Orb2 aggregation enhances memory, we sought to determine where Orb2 aggregates in the adult brain. To visualize and quantify Orb2-aggregation in vivo, we used an assay that reconstitutes the TEV protease activity upon Orb2 aggregation [55]. In this assay, the TEV protease is split into N-terminal (TEVN) and C-terminal (TEVC) halves and fused at the C-terminal end of Orb2 (Figure 6A). The co-expression of Orb2-TEVN and Orb2-TEVC reconstitutes TEV protease activity, and the reconstituted TEV protease can act on a variety of substrates bearing a TEV protease site (Figure 6A). The substrates were cleaved only when both Orb2-TEVN and Orb2-TEVC were present, whereas expression of them separately, mutation of TEV-N catalytic domain (TEVD81N) [56], or TEVN+TEVC without attachment to Orb2 did not have measurable enzymatic activity (Figure 6B; data not shown).

To determine whether this system could be used in the adult fly brain, we replaced the endogenous Orb2 with a genomic fragment of one copy of Orb2-TEVN and one copy of Orb2-TEVC (Figure 6A). To measure Orb2-splitTEV reconstitution, we used a destabilized luciferase [57], in which luciferase is fused to FKBP destabilizing domain (DD) with a TEV protease site in between (Figure 6A). The FKBP-DD-luciferase had a very low activity compared to luciferase alone, and expression of TEV protease

or Orb2-mediated reconstitution of TEV protease resulted in a significant increase of luciferase activity in the brain (Figures 6C and 6D). The increase in luciferase activity was observed only with wild-type constructs ($p = 0.002$), but not in controls (Figure 6D). Furthermore, tyramine, which enhances Orb2 aggregation [26], also significantly increased luciferase activity only in Orb2-TEVN/Orb2-TEVC flies, but not in aggregation-defective Orb2 Δ A-TEVN/Orb2 Δ A-TEVC flies (Figure S6A). These observations suggest that Orb2 can reconstitute TEV protease activity in vitro and in vivo and TEV protease activity can be a proxy for Orb2 aggregation.

Extent of Orb2 Aggregation in the γ Lobe of Mushroom Body Is Predictive of Memory Strength

The luciferase assay did not reveal where Orb2 aggregates. Therefore, to visualize and to quantify Orb2-splitTEV reconstitution in vivo, we developed a GFP-based TEV protease reporter, GFP-dark (Figure 6A). In GFP-dark, a small quenching peptide, which diminishes GFP fluorescence [58], is attached to the C terminus end with an intervening TEV-cleavage site; expression of TEV, and thus removal of the quenching peptide, resulted in significant increase in GFP fluorescence (Figures 6E and S6B–S6D). Importantly, both GFP-dark and GFP have half-lives of ~ 5 hr in the fly brain, allowing for a more dynamic readout of TEV protease activity. There was a higher GFP signal in the mushroom body γ lobe, but not in α/α' and β/β' lobes, in Orb2-TEVN/Orb2-TEVC flies compared to controls (Figure 6F), consistent with other study that Orb2 functions in the mushroom body γ lobe for memory beyond 1 day [24, 59].

To determine the relationship between Orb2 aggregation and memory strength (if any), we used the courtship-suppression paradigm, as it is a single-fly memory assay and memory is scored linearly, providing a spectrum of memory strength. We trained GFP-dark; Orb2-TEVN/Orb2-TEVC flies and tested memory after 1 day. Immediately after testing, the trained and mock-trained fly brains were imaged (Figure 7A) and the courtship-suppression index (indicative of memory strength) and normalized GFP signal in the γ lobe were plotted (please see the Experimental Procedures for details). We observed a significant positive correlation ($p = 0.0014$) between courtship-suppression index and GFP fluorescence in the γ lobe of trained flies (Figures 7B and 7C). No positive correlation was observed following: (1) mock training (Figures 7D and S6E) or after training that produces only short-term memory (Figure 7E); (2) flies expressing only one-half of TEV (ElavGal4::UAS-GFP-dark; Orb2-TEVN/Orb2; Figure 7F); or (3) flies expressing both halves of TEV but a GFP reporter that does not depend on TEV protease activity (ElavGal4::UAS-GFP; Orb2-TEVN/Orb2-TEVC; Figure S6F). A Monte Carlo simulation indicated that the correlation is significantly higher than expected by random chance (Figure S6G). Taken together, these results suggest that Orb2

(D) JJJ2 enhances Orb2 aggregation-dependent translation. Left: schematic of the in vitro translation assay using *Drosophila* embryo extract. JJJ2 mRNA (purple), Orb2A320 mRNA (green), and JJJ2 + Orb2A320 mRNA (brown) were translated in vitro and then incubated with wild-type or $\Delta orb2$ embryo extract as control for 24 hr to allow for conformational alteration of monomeric Orb2B protein in the embryo extract. The mix was then added into $\Delta orb2$ embryo extract containing reporter mRNAs to measure translation. Right: values of firefly luciferase/Renilla luciferase of each group were normalized to control mRNA group, and each experiment is comprised of three independent repeats. Statistical significance was determined using one-way ANOVA for multiple groups, and data are expressed as mean \pm SEM.

* $p < 0.05$, ** $p < 0.01$, and *** $p < 0.001$. See also Figures S2–S4.

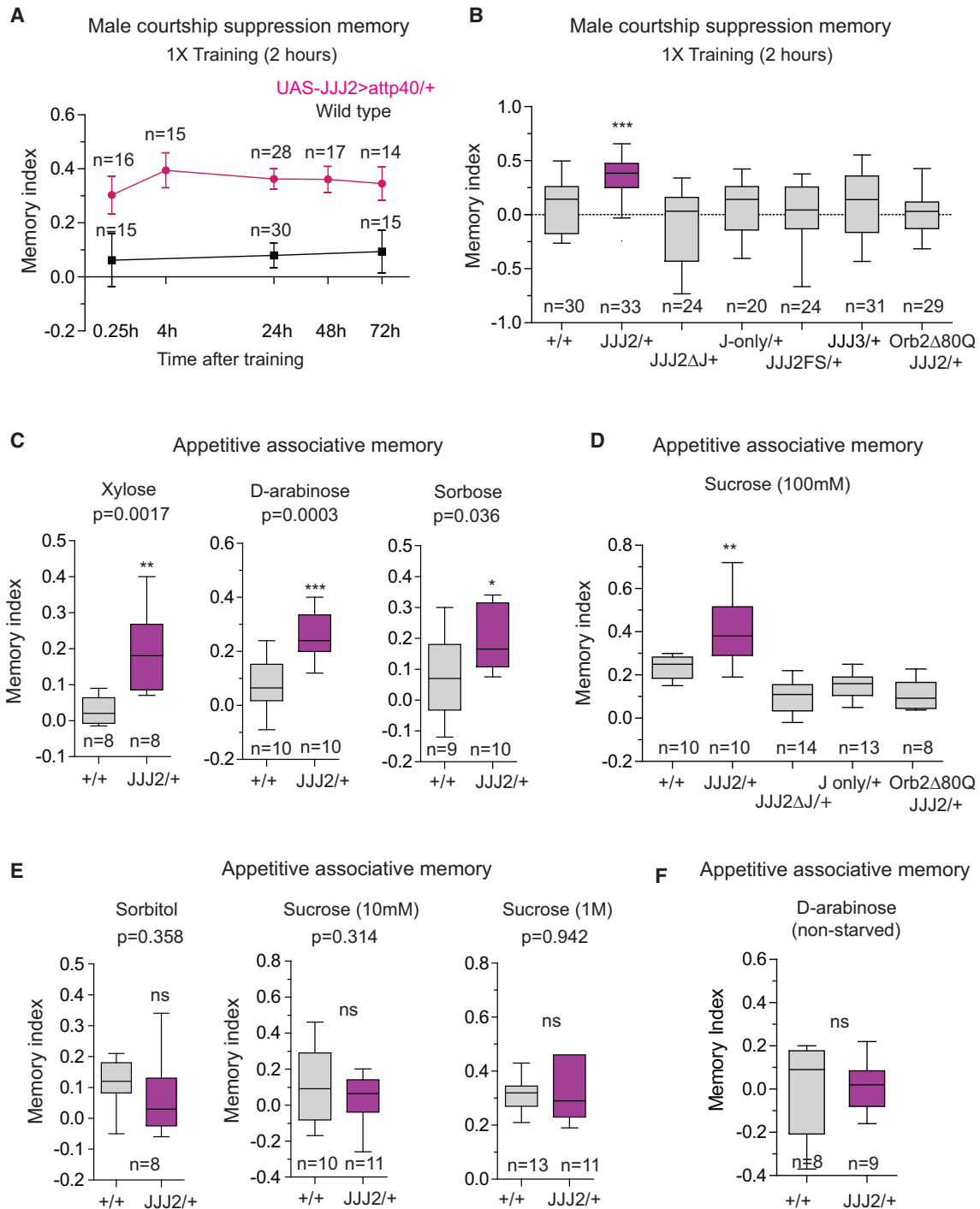


Figure 5. JJJ2 Enhances Long-Term Memory

(A) JJJ2-expressing flies form better long-term memory after suboptimal courtship-suppression training. Wild-type (gray) and UAS-JJJ2-HA>attP40 (purple) flies were subjected to 1× male courtship-suppression training session, and memory was tested at indicated time after training.

(B) Memory enhancement following 1× training requires full-length JJJ2 and is Orb2 dependent.

(C) JJJ2-expressing flies form better appetitive-associative memory. In the appetitive associative memory paradigm, flies were trained to associate odors MCH or OCT with sweet sugars (US), such as 1 M xylose, 1 M D-arabinose, or 1 M sorbose.

(D) Memory enhancement requires full-length JJJ2. 100mM sucrose was used as a subthreshold unconditional stimuli.

(legend continued on next page)

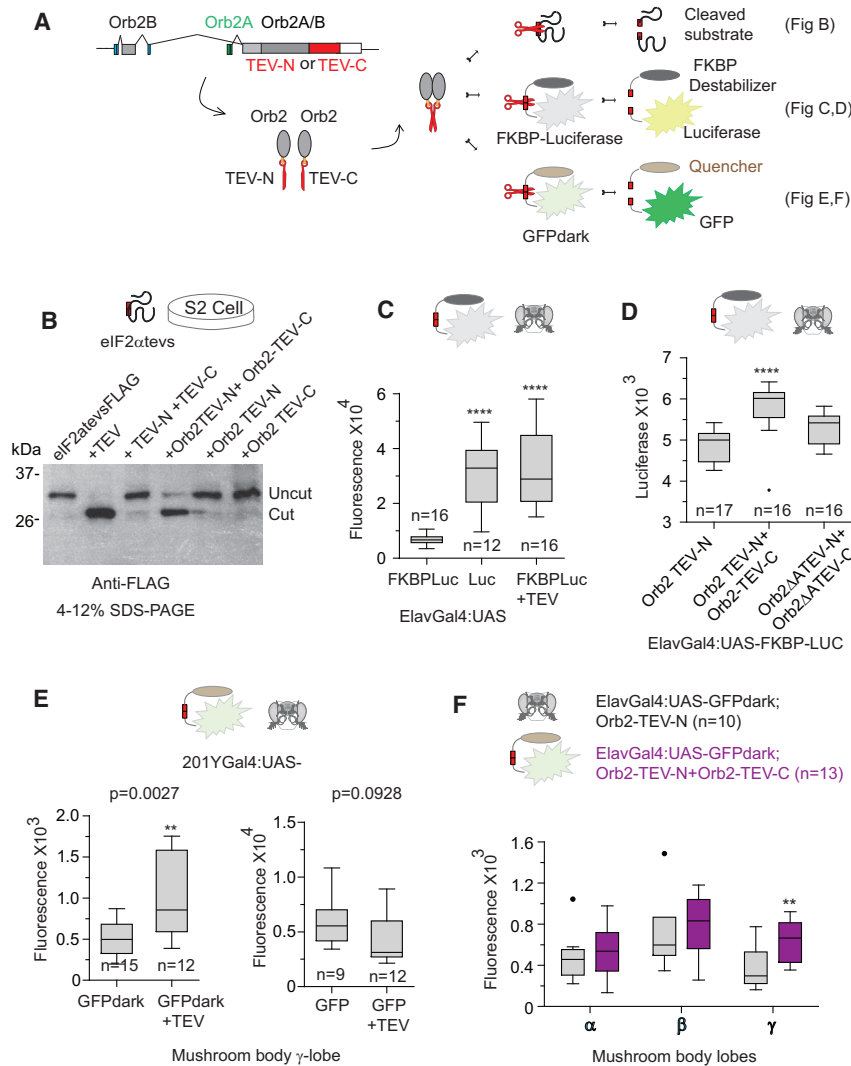


Figure 6. Orb2 Aggregation Reconstitutes TEV Protease Activity

(A) Schematic of Orb2 aggregation-dependent TEV protease reconstitution assay. Endogenous Orb2 is replaced by one copy of Orb2-TEVN and one copy of Orb2-TEVC genomic fragment. Different proteins bearing TEV protease recognition sequence (tevS) were tested. The FKBP-DD-luciferase reporter is comprised of FKBP destabilize domain fused to firefly luciferase (dsLuciferase) with tevS in between. The reporter GFP-dark is comprised of a GFP attached to a quenching peptide with tevS in between.

(B) FLAG-tagged eIF2α-tevS was expressed in S2 cells with the indicated constructs. Western blot was probed for FLAG to detect uncut and cut fragments of eIF2α. Only Orb2TEVN + Orb2TEVC combination resulted in cleavage as efficient as full-length TEV.

(C) In adult fly head, FKBP-DD-luciferase or luciferase was expressed panneuronally using ElavGal4. Co-expression of TEV protease with FKBP-DD-luciferase resulted in significantly more luciferase activity compared to FKBP-DD-luciferase only.

(D) Reconstitution of TEV protease activity in the adult fly head. FKBP-DD-luciferase was expressed panneuronally on the genetic background of Orb2-TEVN+, Orb2-TEVN/Orb2-TEVC, or Orb2ΔA-TEVN/Orb2ΔA-TEVC. Statistical significance was determined using one-way ANOVA.

(E) Fluorescence intensity from the GFP-dark reporter, but not from GFP reporter, is enhanced upon expression of TEV protease in the mushroom body neurons.

(F) When GFP-dark reporter is expressed panneuronally using ElavGal4, fluorescence intensity is significantly higher in the mushroom body γ lobe neuron in Orb2-TEVN/Orb2TEVC flies than in Orb2-TEVN/+ flies. Data are expressed as mean ± SEM, and statistical significance was determined using unpaired t test for two groups.

*p < 0.05, **p < 0.01, and ***p < 0.001. See also Figure S6.

aggregation in the γ lobe neurons is indeed predictive of the memory strength.

The positive correlation between Orb2 aggregation and memory of specific experience is somewhat surprising, considering memory of past experiences and the uncertainty in behavioral manifestation of memory—flies may have memory but decide to act differently or by chance display a behavior that is consistent with memory-driven behavior. In spite of these “noises,” significant positive correlation with long-term memory suggests, at least in *Drosophila*, Orb2 aggregation is most likely a rare process engaged only when an animal forms long-lasting memory. What confers such specificity to this molecular process is of particular interest.

DISCUSSION

A memory, in addition to being stored, must be accessed, retrieved, and able to elicit the proper behavioral response, and perturbation of any of these steps can interfere with behavioral display of memory. Whereas previous studies have found prion-like domain [24, 25] and aggregation of Orb2 [26] is required for memory, it is unclear when and how long Orb2 activity is required and whether Orb2 aggregation is one of the limiting steps in memory formation. Here, by acutely and reversibly inactivating Orb2 at different stages of memory only in the adult neurons, by artificially facilitating Orb2 aggregation, and by visualizing aggregated Orb2 following behavioral training, we find

(E) JJJ2 does not have any effect on stimuli that produce robust long-term memory or no memory. Sorbitol, a non-sweet sugar, or 10 mM sucrose was used as a weak stimuli and 1 M sucrose as a strong stimuli.

(F) JJJ2 does not enhance memory in non-starved flies in appetitive-associative memory. Data are expressed as mean ± SEM, and statistical significance was determined using one-way ANOVA for multiple groups and unpaired t test for two groups.

*p < 0.05, **p < 0.01, and ***p < 0.001. See also Figure S5.

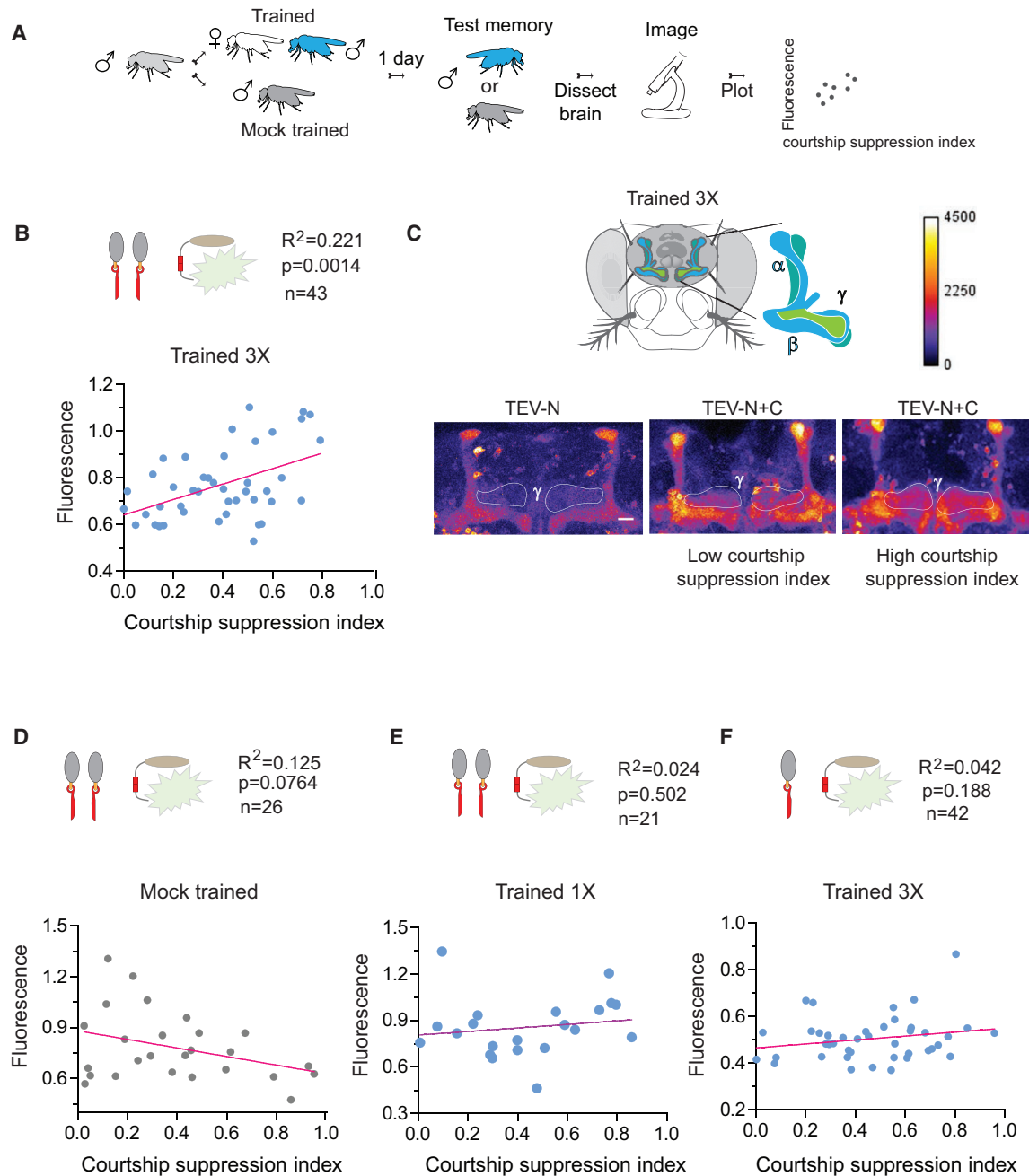


Figure 7. Orb2 Aggregation in the γ Lobe of Mushroom Body Is Predictive of Memory Strength

(A) GFP-dark reporter was expressed panneuronally using ElavGal4 in the Orb2-TEVN/Orb2-TEVC flies. Trained or mock-trained male flies were tested for memory at 24 hr, and immediately after testing, brains were dissected and imaged.

(B) In 3x trained flies (ElavGal4::UAS-GFPdark; Orb2-TEVN/Orb2-TEVC), memory is positively correlated with GFP intensity in γ lobe.

(C) Heatmap images represent GFP signals in the mushroom body region of the following groups: control Orb2-TEVN/Orb2 (left), Orb2-TEVN/Orb2-TEVC low courtship suppression (middle), and high courtship suppression (right). The γ lobe region is outlined. The scale bar represents 20 μ m.

(D–F) Control groups do not show positive correlation between courtship suppression and GFP intensity in γ lobe: (D) mock-trained flies (ElavGal4::UAS-GFPdark; Orb2-TEVN/Orb2-TEVC); (E) 1x trained flies (ElavGal4::UAS-GFPdark; Orb2-TEVN/Orb2-TEVC); and (F) 3x trained flies with one-half of TEV protease (ElavGal4::UAS-GFPdark; Orb2-TEVN/Orb2). Linear regression was used to analyze the correlation between courtship-suppression index and GFP intensity. Only the positive courtship-suppression index was plotted.

See also [Figure S6](#) and [Table S1](#).

that Orb2 is required for the formation, persistent storage, and retrieval/expression of memory, that facilitation of Orb2 aggregation facilitates long-lasting memory formation, and that the extent of Orb2 aggregation in the γ lobe neurons is predictive of memory strength. As we discuss below, taken together with studies in *Aplysia* [21, 22], fly [25, 26, 30], and in mouse [19, 27], these observations could be best explained if one considers that self-sustaining aggregates of CPEB are constituents of the memory engram.

Aggregated CPEB/Orb2 as a Putative Memory Engram

How could an aggregated state of a protein synthesis regulator explain formation, retrieval, and, under certain circumstances, recovery of memory? We postulate that activity-dependent conformational switch to the aggregated state creates a biochemical state that is necessary to store memory, and either access to or activity of this aggregated state is necessary to recall/express memory. Because these are the very same properties that are assigned to a physical substrate of memory, a.k.a. memory engram, we deem that involvement of Orb2 in memory can be best encapsulated if one considers it as a memory engram. We do not intend to say that aggregated Orb2 per se represents a memory, rather it is a biochemical state that helps to create and maintain an altered activity state of a network of neurons, which represents a memory.

Because aggregation of Orb2 enhances translation [31], we postulate that the aggregated Orb2 allows the synapse to maintain its altered state by continuously capturing and translating specific mRNAs at the activated synapse. Therefore, inactivation of Orb2 any time after memory formation interferes with the expression of memory. When Orb2 is inactivated/reduced during encoding, memory cannot be recovered with newly synthesized Orb2 because the conformational switch to the aggregated state never took place and no long-term memory was formed. On the other hand, facilitation of Orb2 aggregation by JJJ2 lowers the threshold for memory formation by allowing suboptimal-training-induced mRNAs, which otherwise would not be utilized by the synapse, to be captured and utilized by the synapse to produce long-term memory.

Memory Recovery

Intriguingly, we find that, once established, specific memory can recover in an Orb2-dependent manner. Although the exact mechanism of memory recovery upon restoration of Orb2 is unclear and we do not know whether, in our experimental manipulation, all of the Orb2-expressing neurons lost 50% of the protein or, in a subset of critical neurons, 100% of the protein is lost, we envision the following possibilities. Small amounts of full-length Orb2 aggregates or aggregates of just the N-terminal domain could induce aggregation of monomeric Orb2 [17, 25, 31]. Therefore, one possibility is that the residual uncleaved aggregated Orb2 or the cleaved aggregated N-terminal domain, although inadequate for full translational activation and expression of memory, reconstitutes the memory trace once monomeric Orb2 protein level is restored. A formal test of this possibility would be if Orb2 aggregates are completely eliminated after memory formation, memory should never recover. Although technically it has not been feasible to accomplish this in *Drosophila*, recent studies in mice are consistent with this possi-

bility: removal of CPEB3 from the genomic locus results in loss of established memory that cannot be rescued by restoring CPEB3 expression after several weeks [27]. The other possibilities are that Orb2 has distinct and independent function in memory storage and memory retrieval. Alternatively, there is some process upstream of Orb2 that regulates Orb2 aggregation—once Orb2 protein level is restored, the aggregation and translation are restored by this upstream process to the level adequate for memory. In all of these scenarios, continued Orb2-dependent translation is required for manifestation of memory days after formation.

Memory Enhancement

We find that JJJ2 can facilitate but cannot initiate long-term memory formation, suggesting that there are restrictions to long-term memory formation and most likely Orb2 aggregation that JJJ2 by itself cannot overcome. Indeed, memory improvement should be a rare phenomenon because, to improve memory, mere activation of a molecular process is not enough—it must be engaged in the right cell (and synapse) at the right amount and requires accompanying changes in other molecular processes. Availability of monomeric Orb2A protein, a substrate of JJJ2, could be one of the restricting components, because it is extremely low abundant [25, 26] and has a very short half-life [28].

Among chaperones, the Hsp40 family of chaperones is most expanded [47]. JJJ2, a low abundant nonessential gene, is reported (*Saccharomyces Genome Database* [SGD]) to interact physically only with four proteins in yeast, suggesting that JJJ2 is likely to have a limited set of targets. Based on the findings that JJJ2 enhances Orb2 aggregation, Orb2-dependent translation, and Orb2-dependent memory, we postulate that JJJ2-Orb2 interaction is important for memory and Orb2 aggregation is at least a rate-limiting step in long-lasting memory formation. However, this does not mean that the memory-enhancing effect of JJJ2 is mediated exclusively through Orb2. Also JJJ2 serves as a tool, but not necessarily provides mechanistic insights into how chaperones control Orb2 aggregation in adult fly brain. However, it raises the possibility that functional protein aggregation in the brain can be guided by molecular chaperones and there may be functional equivalent of JJJ2 in *Drosophila* and other species.

Visualization of Molecular Signature of a Long-Lasting Memory

An independent measure of memory in addition to behavioral readout is necessary to interrogate the mechanism of persistence as well as decay of memory. Previously, memory traces have been visualized at neuronal activity level using immediate early gene [11, 12, 60–64] or calcium sensors [59, 65–67]. Likewise, autocatalytic calcium calmodulin-dependent kinase II (CamKII) [68], a specific isoform of atypical protein kinase C, PKM ζ [69], the ratio of phosphorylated-CREB to total CREB or the level of postsynaptic GluR2 [70], and DNA modification [71] have been reported as biochemical substrates of long-term memory. However, some of these molecules are involved in a broad range of physiological functions, rendering them difficult to always associate with memory processes per se. The specific involvement of CPEB/Orb2 aggregates perhaps

provides a more selective tool for “visualization” of memory, at least in *Drosophila*.

The *Drosophila* mushroom body is generally believed to be important for long-lasting memory [8, 72]. Approximately 2,000 neurons in the mushroom body are divided into three distinct lobes (α/β , α'/β' , and γ) and seven distinct cell types [73, 74]. Multiple studies suggest the vertical branch of α/β lobe is required for memory persisting for 9–24 hr [67, 75, 76], whereas the γ lobe is important for memory beyond 1 day (18–48 hr) [24, 59]. We find aggregated Orb2 in the γ lobe is positively correlated with memory strength. It is unclear how many neurons or whether a specific set of neurons in the γ lobe is recruited for a given memory. Likewise, although Orb2 aggregation in the γ lobe is predictive of long-term memory, Orb2 does not necessarily only aggregate in the γ lobe. Nonetheless it can serve as a molecular signature of memory and offers a possibility to interrogate the molecular basis of memory loss.

EXPERIMENTAL PROCEDURES

Please see the [Supplemental Information](#) for details of the methods.

SUPPLEMENTAL INFORMATION

Supplemental Information includes Supplemental Experimental Procedures, six figures, and one table and can be found with this article online at <http://dx.doi.org/10.1016/j.cub.2016.09.054>.

AUTHOR CONTRIBUTIONS

K.S. and L.L. conceived of the project, designed the experiments, analyzed the data, and prepared the manuscript. L.L., Y.Z., B.D.S., J.R.U., M.R.K., and C.P.S. performed the experiments. J.R.U., B.D.S., and B.R. assisted with imaging and analysis. K.S. and L.L. wrote the paper and made the figures.

ACKNOWLEDGMENTS

We thank Sarah Smith and Zulin Yu of the Stowers Microscopy Center for their help in imaging. We thank the K.S. lab members for discussions. We thank Fengzhen Ren and Soham Karmakar for technical assistance in biochemical experiments. This work was supported by the Stowers Institute for Medical Research and a NIH R01 grant (no. MH101440-01A1).

Received: July 14, 2016

Revised: September 22, 2016

Accepted: September 26, 2016

Published: November 3, 2016

REFERENCES

1. Semon, R. (1921). The Mneme (Allen & Unwin).
2. Dudai, Y. (2012). The restless engram: consolidations never end. *Annu. Rev. Neurosci.* **35**, 227–247.
3. Tonegawa, S., Pignatelli, M., Roy, D.S., and Ryan, T.J. (2015). Memory engram storage and retrieval. *Curr. Opin. Neurobiol.* **35**, 101–109.
4. Penfield, W. (1968). Engrams in the human brain. *Mechanisms of memory. Proc. R. Soc. Med.* **61**, 831–840.
5. Mayford, M., Siegelbaum, S.A., and Kandel, E.R. (2012). Synapses and memory storage. *Cold Spring Harb. Perspect. Biol.* **4**, a005751.
6. Takeuchi, T., Duszkiwicz, A.J., and Morris, R.G. (2013). The synaptic plasticity and memory hypothesis: encoding, storage and persistence. *Philos. Trans. R. Soc. Lond. B Biol. Sci.* **369**, 20130288.
7. Davis, R.L. (2011). Traces of *Drosophila* memory. *Neuron* **70**, 8–19.
8. Guven-Ozkan, T., and Davis, R.L. (2014). Functional neuroanatomy of *Drosophila* olfactory memory formation. *Learn. Mem.* **21**, 519–526.
9. Cowansage, K.K., Shuman, T., Dillingham, B.C., Chang, A., Golshani, P., and Mayford, M. (2014). Direct reactivation of a coherent neocortical memory of context. *Neuron* **84**, 432–441.
10. Garner, A.R., Rowland, D.C., Hwang, S.Y., Baumgaertel, K., Roth, B.L., Kentros, C., and Mayford, M. (2012). Generation of a synthetic memory trace. *Science* **335**, 1513–1516.
11. Liu, X., Ramirez, S., Pang, P.T., Puryear, C.B., Govindarajan, A., Deisseroth, K., and Tonegawa, S. (2012). Optogenetic stimulation of a hippocampal engram activates fear memory recall. *Nature* **484**, 381–385.
12. Ramirez, S., Liu, X., Lin, P.A., Suh, J., Pignatelli, M., Redondo, R.L., Ryan, T.J., and Tonegawa, S. (2013). Creating a false memory in the hippocampus. *Science* **341**, 387–391.
13. Josselyn, S.A., Köhler, S., and Frankland, P.W. (2015). Finding the engram. *Nat. Rev. Neurosci.* **16**, 521–534.
14. Ho, V.M., Lee, J.A., and Martin, K.C. (2011). The cell biology of synaptic plasticity. *Science* **334**, 623–628.
15. Richter, J.D., and Klann, E. (2009). Making synaptic plasticity and memory last: mechanisms of translational regulation. *Genes Dev.* **23**, 1–11.
16. Nader, K. (2015). Reconsolidation and the dynamic nature of memory. *Cold Spring Harb. Perspect. Biol.* **7**, a021782.
17. Hervás, R., Li, L., Majumdar, A., Fernández-Ramírez, Mdel.C., Unruh, J.R., Slaughter, B.D., Galera-Prat, A., Santana, E., Suzuki, M., Nagai, Y., et al. (2016). Molecular basis of Orb2 amyloidogenesis and blockade of memory consolidation. *PLoS Biol.* **14**, e1002361.
18. Si, K., Lindquist, S., and Kandel, E.R. (2003). A neuronal isoform of the aplysia CPEB has prion-like properties. *Cell* **115**, 879–891.
19. Stephan, J.S., Fioriti, L., Lamba, N., Colnaghi, L., Karl, K., Derkach, I.L., and Kandel, E.R. (2015). The CPEB3 protein is a functional prion that interacts with the actin cytoskeleton. *Cell Rep.* **11**, 1772–1785.
20. Heinrich, S.U., and Lindquist, S. (2011). Protein-only mechanism induces self-perpetuating changes in the activity of neuronal Aplysia cytoplasmic polyadenylation element binding protein (CPEB). *Proc. Natl. Acad. Sci. USA* **108**, 2999–3004.
21. Miniaci, M.C., Kim, J.H., Puthanveetil, S.V., Si, K., Zhu, H., Kandel, E.R., and Bailey, C.H. (2008). Sustained CPEB-dependent local protein synthesis is required to stabilize synaptic growth for persistence of long-term facilitation in Aplysia. *Neuron* **59**, 1024–1036.
22. Si, K., Choi, Y.B., White-Grindley, E., Majumdar, A., and Kandel, E.R. (2010). Aplysia CPEB can form prion-like multimers in sensory neurons that contribute to long-term facilitation. *Cell* **140**, 421–435.
23. Si, K., Giustetto, M., Etkin, A., Hsu, R., Janisiewicz, A.M., Miniaci, M.C., Kim, J.H., Zhu, H., and Kandel, E.R. (2003). A neuronal isoform of CPEB regulates local protein synthesis and stabilizes synapse-specific long-term facilitation in aplysia. *Cell* **115**, 893–904.
24. Keleman, K., Krüttner, S., Alenius, M., and Dickson, B.J. (2007). Function of the *Drosophila* CPEB protein Orb2 in long-term courtship memory. *Nat. Neurosci.* **10**, 1587–1593.
25. Krüttner, S., Stepien, B., Noordermeer, J.N., Mommaas, M.A., Mechtler, K., Dickson, B.J., and Keleman, K. (2012). *Drosophila* CPEB Orb2A mediates memory independent of its RNA-binding domain. *Neuron* **76**, 383–395.
26. Majumdar, A., Cesario, W.C., White-Grindley, E., Jiang, H., Ren, F., Khan, M.R., Li, L., Choi, E.M., Kannan, K., Guo, F., et al. (2012). Critical role of amyloid-like oligomers of *Drosophila* Orb2 in the persistence of memory. *Cell* **148**, 515–529.
27. Fioriti, L., Myers, C., Huang, Y.Y., Li, X., Stephan, J.S., Trifilieff, P., Colnaghi, L., Kosmidis, S., Drisaldi, B., Pavlopoulos, E., and Kandel, E.R. (2015). The persistence of hippocampal-based memory requires protein synthesis mediated by the prion-like protein CPEB3. *Neuron* **86**, 1433–1448.

28. White-Grindley, E., Li, L., Mohammad Khan, R., Ren, F., Saraf, A., Florens, L., and Si, K. (2014). Contribution of Orb2A stability in regulated amyloid-like oligomerization of *Drosophila* Orb2. *PLoS Biol.* *12*, e1001786.
29. Xu, S., Hafer, N., Agunwamba, B., and Schedl, P. (2012). The CPEB protein Orb2 has multiple functions during spermatogenesis in *Drosophila melanogaster*. *PLoS Genet.* *8*, e1003079.
30. Krüttner, S., Traunmüller, L., Dag, U., Jandrasits, K., Stepien, B., Iyer, N., Fradkin, L.G., Noordermeer, J.N., Mensh, B.D., and Keleman, K. (2015). Synaptic Orb2A bridges memory acquisition and late memory consolidation in *Drosophila*. *Cell Rep.* *11*, 1953–1965.
31. Khan, M.R., Li, L., Pérez-Sánchez, C., Saraf, A., Florens, L., Slaughter, B.D., Unruh, J.R., and Si, K. (2015). Amyloidogenic oligomerization transforms *Drosophila* Orb2 from a translation repressor to an activator. *Cell* *163*, 1468–1483.
32. Mastushita-Sakai, T., White-Grindley, E., Samuelson, J., Seidel, C., and Si, K. (2010). *Drosophila* Orb2 targets genes involved in neuronal growth, synapse formation, and protein turnover. *Proc. Natl. Acad. Sci. USA* *107*, 11987–11992.
33. Dougherty, W.G., Cary, S.M., and Parks, T.D. (1989). Molecular genetic analysis of a plant virus polyprotein cleavage site: a model. *Virology* *171*, 356–364.
34. Roman, G., Endo, K., Zong, L., and Davis, R.L. (2001). P[Switch], a system for spatial and temporal control of gene expression in *Drosophila melanogaster*. *Proc. Natl. Acad. Sci. USA* *98*, 12602–12607.
35. McGuire, S.E., Mao, Z., and Davis, R.L. (2004). Spatiotemporal gene expression targeting with the TARGET and gene-switch systems in *Drosophila*. *Sci. STKE* *2004*, pl6.
36. McBride, S.M., Giuliani, G., Choi, C., Krause, P., Correale, D., Watson, K., Baker, G., and Siwicki, K.K. (1999). Mushroom body ablation impairs short-term memory and long-term memory of courtship conditioning in *Drosophila melanogaster*. *Neuron* *24*, 967–977.
37. Siegel, R.W., and Hall, J.C. (1979). Conditioned responses in courtship behavior of normal and mutant *Drosophila*. *Proc. Natl. Acad. Sci. USA* *76*, 3430–3434.
38. Kacsoh, B.Z., Bozler, J., Hodge, S., Ramaswami, M., and Bosco, G. (2015). A novel paradigm for nonassociative long-term memory in *Drosophila*: predator-induced changes in oviposition behavior. *Genetics* *199*, 1143–1157.
39. Krashes, M.J., and Waddell, S. (2008). Rapid consolidation to a radish and protein synthesis-dependent long-term memory after single-session appetitive olfactory conditioning in *Drosophila*. *J. Neurosci.* *28*, 3103–3113.
40. Tempel, B.L., Bonini, N., Dawson, D.R., and Quinn, W.G. (1983). Reward learning in normal and mutant *Drosophila*. *Proc. Natl. Acad. Sci. USA* *80*, 1482–1486.
41. Pai, T.P., Chen, C.C., Lin, H.H., Chin, A.L., Lai, J.S., Lee, P.T., Tully, T., and Chiang, A.S. (2013). *Drosophila* ORB protein in two mushroom body output neurons is necessary for long-term memory formation. *Proc. Natl. Acad. Sci. USA* *110*, 7898–7903.
42. Kim, Y.E., Hipp, M.S., Bracher, A., Hayer-Hartl, M., and Hartl, F.U. (2013). Molecular chaperone functions in protein folding and proteostasis. *Annu. Rev. Biochem.* *82*, 323–355.
43. Cashikar, A.G., Duennwald, M., and Lindquist, S.L. (2005). A chaperone pathway in protein disaggregation. Hsp26 alters the nature of protein aggregates to facilitate reactivation by Hsp104. *J. Biol. Chem.* *280*, 23869–23875.
44. Vacher, C., Garcia-Oroz, L., and Rubinsztein, D.C. (2005). Overexpression of yeast hsp104 reduces polyglutamine aggregation and prolongs survival of a transgenic mouse model of Huntington's disease. *Hum. Mol. Genet.* *14*, 3425–3433.
45. Gong, Y., Kakihara, Y., Krogan, N., Greenblatt, J., Emili, A., Zhang, Z., and Houry, W.A. (2009). An atlas of chaperone-protein interactions in *Saccharomyces cerevisiae*: implications to protein folding pathways in the cell. *Mol. Syst. Biol.* *5*, 275.
46. Gillies, A.T., Taylor, R., and Gestwicki, J.E. (2012). Synthetic lethal interactions in yeast reveal functional roles of J protein co-chaperones. *Mol. Biosyst.* *8*, 2901–2908.
47. Kampinga, H.H., and Craig, E.A. (2010). The HSP70 chaperone machinery: J proteins as drivers of functional specificity. *Nat. Rev. Mol. Cell Biol.* *11*, 579–592.
48. Troisi, E.M., Rockman, M.E., Nguyen, P.P., Oliver, E.E., and Hines, J.K. (2015). Swa2, the yeast homolog of mammalian auxilin, is specifically required for the propagation of the prion variant [URE3-1]. *Mol. Microbiol.* *97*, 926–941.
49. Hines, J.K., Li, X., Du, Z., Higurashi, T., Li, L., and Craig, E.A. (2011). [SWI], the prion formed by the chromatin remodeling factor Swi1, is highly sensitive to alterations in Hsp70 chaperone system activity. *PLoS Genet.* *7*, e1001309.
50. Brand, A.H., and Perrimon, N. (1993). Targeted gene expression as a means of altering cell fates and generating dominant phenotypes. *Development* *118*, 401–415.
51. Kesti, T., McDonald, W.H., Yates, J.R., 3rd, and Wittenberg, C. (2004). Cell cycle-dependent phosphorylation of the DNA polymerase epsilon subunit, Dpb2, by the Cdc28 cyclin-dependent protein kinase. *J. Biol. Chem.* *279*, 14245–14255.
52. Burke, C.J., and Waddell, S. (2011). Remembering nutrient quality of sugar in *Drosophila*. *Curr. Biol.* *21*, 746–750.
53. Colomb, J., Kaiser, L., Chabaud, M.A., and Preat, T. (2009). Parametric and genetic analysis of *Drosophila* appetitive long-term memory and sugar motivation. *Genes Brain Behav.* *8*, 407–415.
54. Putz, G., and Heisenberg, M. (2002). Memories in *Drosophila* heat-box learning. *Learn. Mem.* *9*, 349–359.
55. Wehr, M.C., Laage, R., Bolz, U., Fischer, T.M., Grünewald, S., Scheek, S., Bach, A., Nave, K.A., and Rossner, M.J. (2006). Monitoring regulated protein-protein interactions using split TEV. *Nat. Methods* *3*, 985–993.
56. Dougherty, W.G., Parks, T.D., Cary, S.M., Bazan, J.F., and Fletterick, R.J. (1989). Characterization of the catalytic residues of the tobacco etch virus 49-kDa proteinase. *Virology* *172*, 302–310.
57. Sellmyer, M.A., Thorne, S.H., Banaszynski, L.A., Contag, C.H., and Wandless, T.J. (2009). A general method for conditional regulation of protein stability in living animals. *Cold Spring Harb. Protoc.* *2009*, pdb.prot5173.
58. Nicholls, S.B., Chu, J., Abbruzzese, G., Tremblay, K.D., and Hardy, J.A. (2011). Mechanism of a genetically encoded dark-to-bright reporter for caspase activity. *J. Biol. Chem.* *286*, 24977–24986.
59. Akalal, D.B., Yu, D., and Davis, R.L. (2010). A late-phase, long-term memory trace forms in the γ neurons of *Drosophila* mushroom bodies after olfactory classical conditioning. *J. Neurosci.* *30*, 16699–16708.
60. Tayler, K.K., Tanaka, K.Z., Reijmers, L.G., and Wiltgen, B.J. (2013). Reactivation of neural ensembles during the retrieval of recent and remote memory. *Curr. Biol.* *23*, 99–106.
61. Tanaka, K.Z., Pevzner, A., Hamidi, A.B., Nakazawa, Y., Graham, J., and Wiltgen, B.J. (2014). Cortical representations are reinstated by the hippocampus during memory retrieval. *Neuron* *84*, 347–354.
62. Redondo, R.L., Kim, J., Arons, A.L., Ramirez, S., Liu, X., and Tonegawa, S. (2014). Bidirectional switch of the valence associated with a hippocampal contextual memory engram. *Nature* *513*, 426–430.
63. Ryan, T.J., Roy, D.S., Pignatelli, M., Arons, A., and Tonegawa, S. (2015). Memory. Engram cells retain memory under retrograde amnesia. *Science* *348*, 1007–1013.
64. Reijmers, L.G., Perkins, B.L., Matsuo, N., and Mayford, M. (2007). Localization of a stable neural correlate of associative memory. *Science* *317*, 1230–1233.
65. Cervantes-Sandoval, I., and Davis, R.L. (2012). Distinct traces for appetitive versus aversive olfactory memories in DPM neurons of *Drosophila*. *Curr. Biol.* *22*, 1247–1252.

66. Yu, D., Keene, A.C., Srivatsan, A., Waddell, S., and Davis, R.L. (2005). *Drosophila* DPM neurons form a delayed and branch-specific memory trace after olfactory classical conditioning. *Cell* 123, 945–957.
67. Yu, D., Akalal, D.B., and Davis, R.L. (2006). *Drosophila* alpha/beta mushroom body neurons form a branch-specific, long-term cellular memory trace after spaced olfactory conditioning. *Neuron* 52, 845–855.
68. Sanhueza, M., and Lisman, J. (2013). The CaMKII/NMDAR complex as a molecular memory. *Mol. Brain* 6, 10.
69. Sacktor, T.C. (2011). How does PKM ζ maintain long-term memory? *Nat. Rev. Neurosci.* 12, 9–15.
70. Miguez, P.V., Hardt, O., Wu, D.C., Gamache, K., Sacktor, T.C., Wang, Y.T., and Nader, K. (2010). PKMzeta maintains memories by regulating GluR2-dependent AMPA receptor trafficking. *Nat. Neurosci.* 13, 630–634.
71. Zovkic, I.B., Guzman-Karlsson, M.C., and Sweatt, J.D. (2013). Epigenetic regulation of memory formation and maintenance. *Learn. Mem.* 20, 61–74.
72. Heisenberg, M. (2003). Mushroom body memoir: from maps to models. *Nat. Rev. Neurosci.* 4, 266–275.
73. Aso, Y., Grübel, K., Busch, S., Friedrich, A.B., Siwanowicz, I., and Tanimoto, H. (2009). The mushroom body of adult *Drosophila* characterized by GAL4 drivers. *J. Neurogenet.* 23, 156–172.
74. Aso, Y., Hattori, D., Yu, Y., Johnston, R.M., Iyer, N.A., Ngo, T.T., Dionne, H., Abbott, L.F., Axel, R., Tanimoto, H., and Rubin, G.M. (2014). The neuronal architecture of the mushroom body provides a logic for associative learning. *eLife* 3, e04577.
75. Krashes, M.J., Keene, A.C., Leung, B., Armstrong, J.D., and Waddell, S. (2007). Sequential use of mushroom body neuron subsets during *Drosophila* odor memory processing. *Neuron* 53, 103–115.
76. Pascual, A., and Pr eat, T. (2001). Localization of long-term memory within the *Drosophila* mushroom body. *Science* 294, 1115–1117.

Current Biology, Volume 26

Supplemental Information

A Putative Biochemical Engram of Long-Term Memory

Liyang Li, Consuelo Perez Sanchez, Brian D. Slaughter, Yubai Zhao, Mohammed Repon Khan, Jay R. Unruh, Boris Rubinstein, and Kausik Si

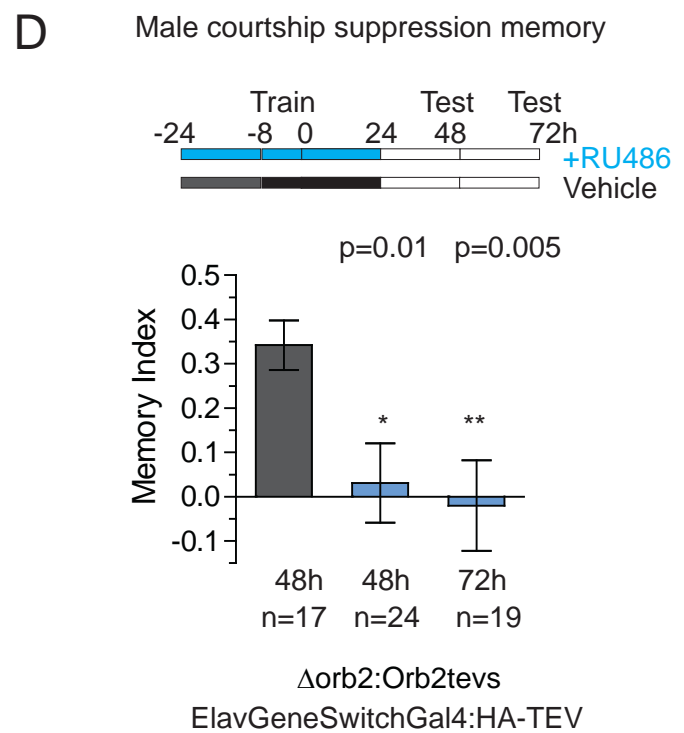
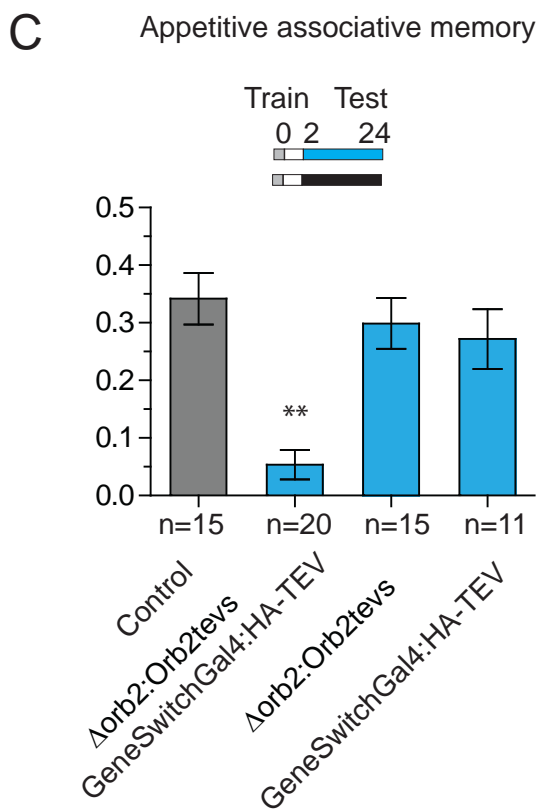
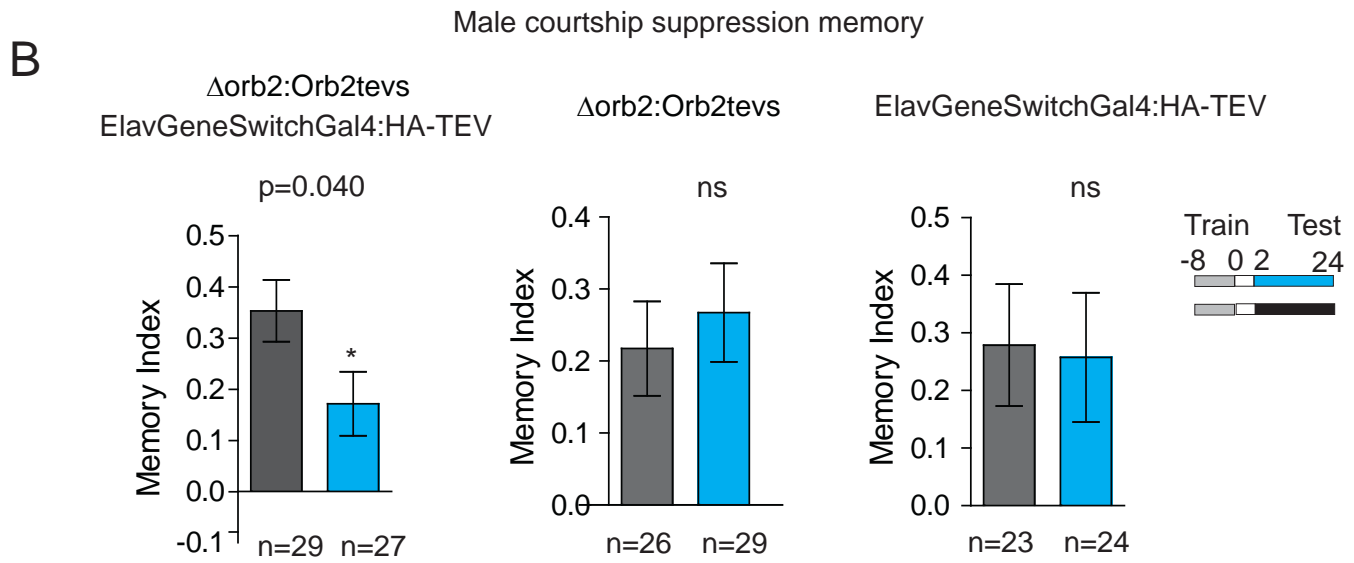
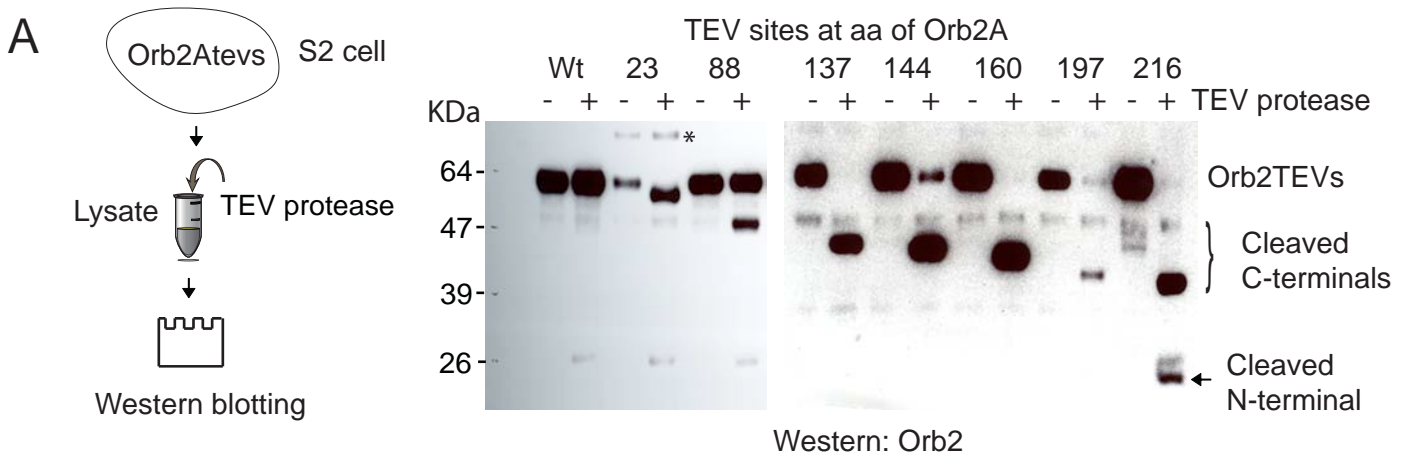


Figure S1

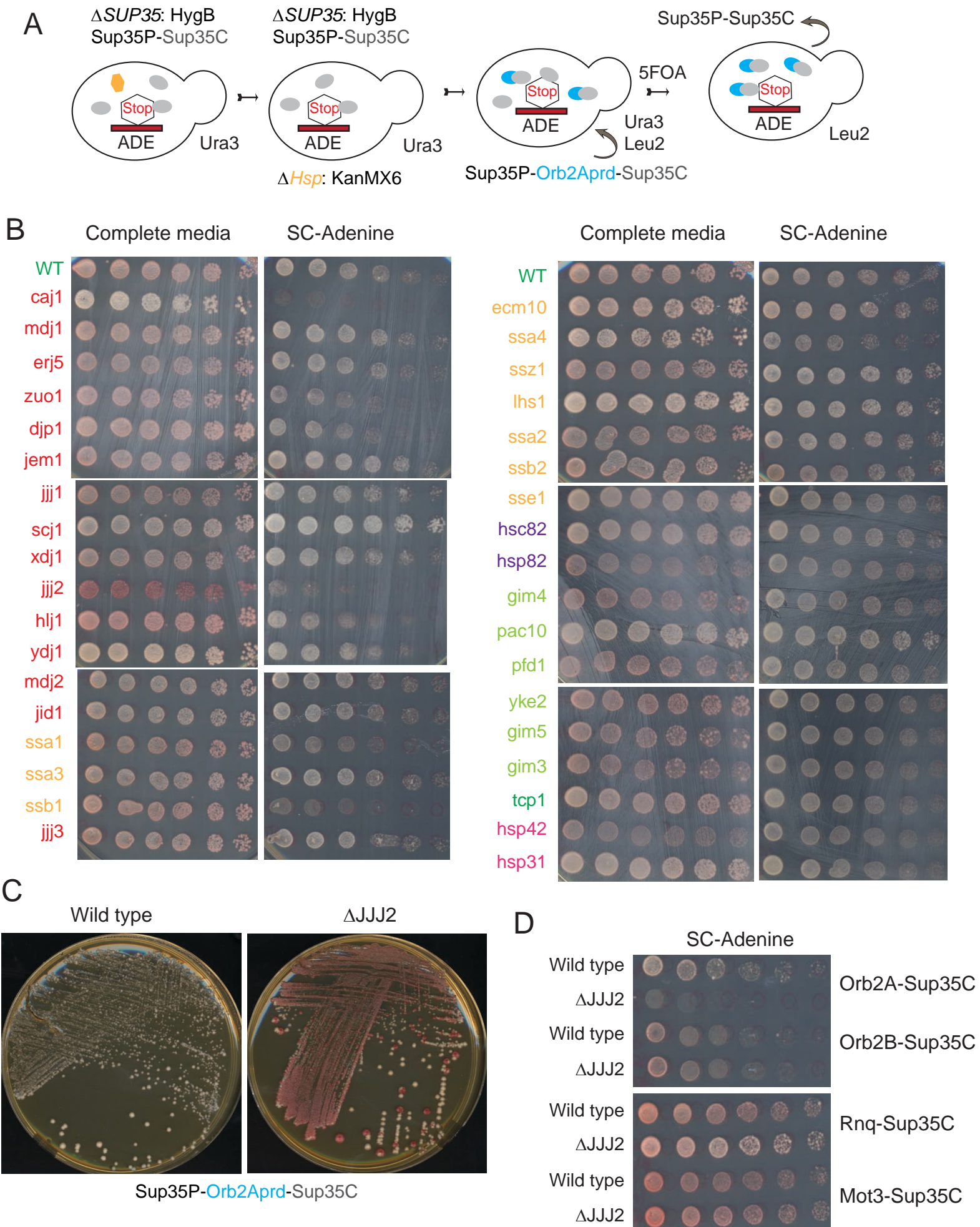


Figure S2

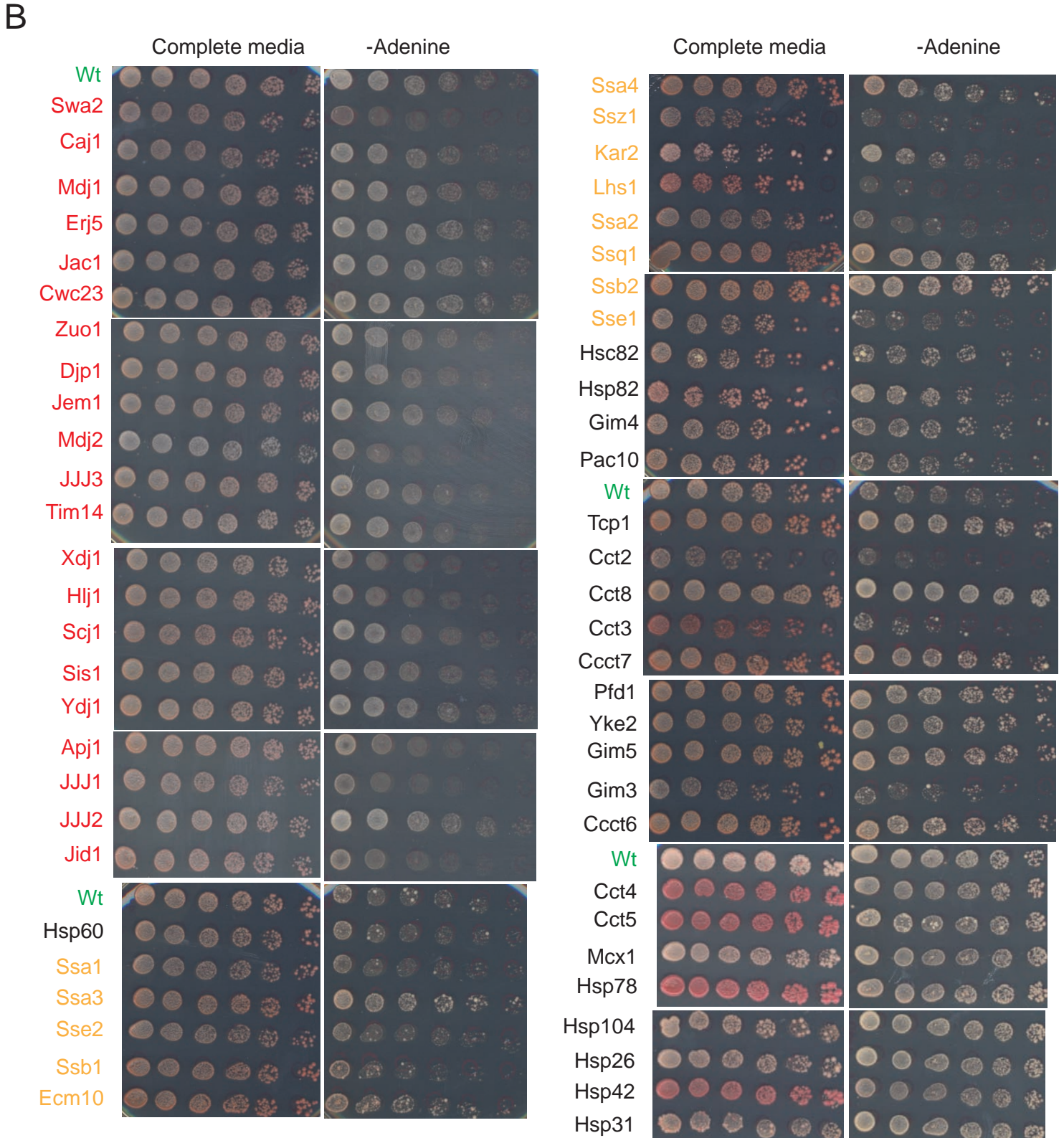
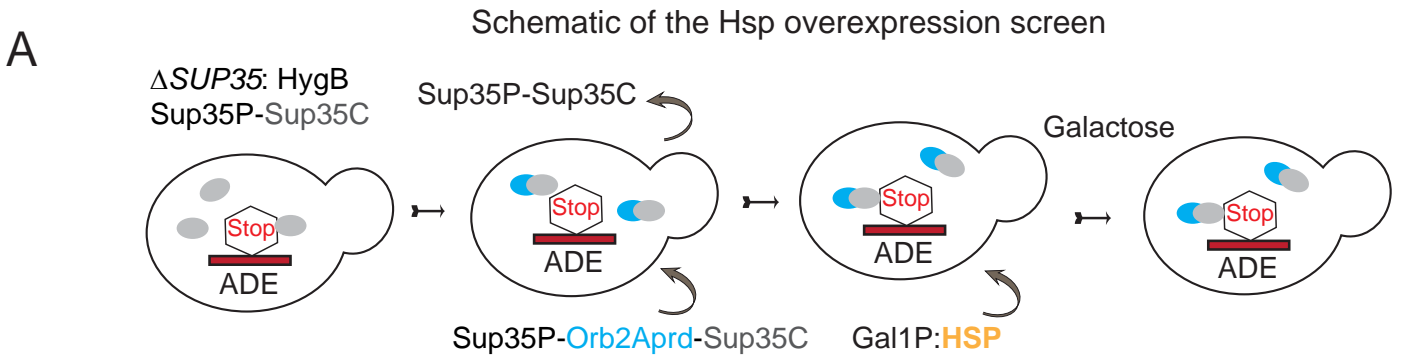
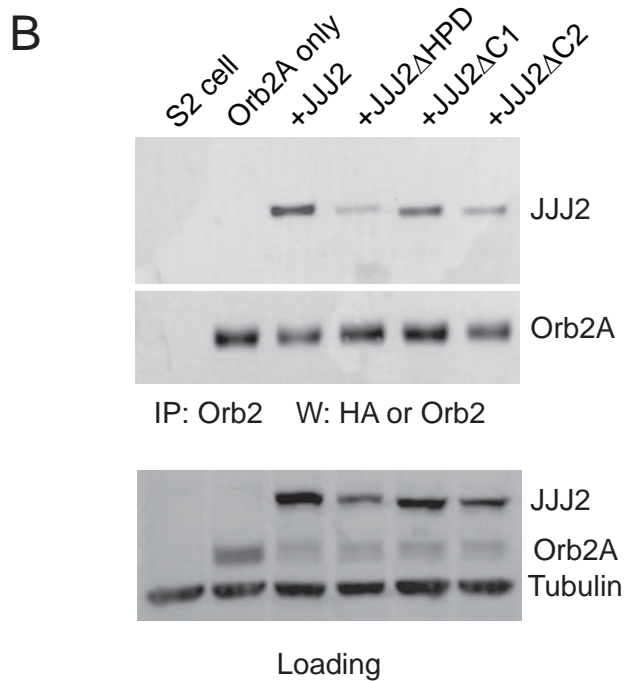
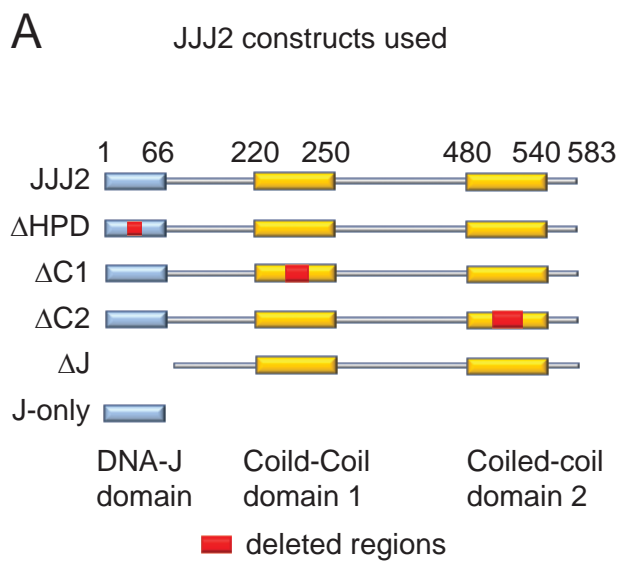


Figure S3



C

Super resolution images

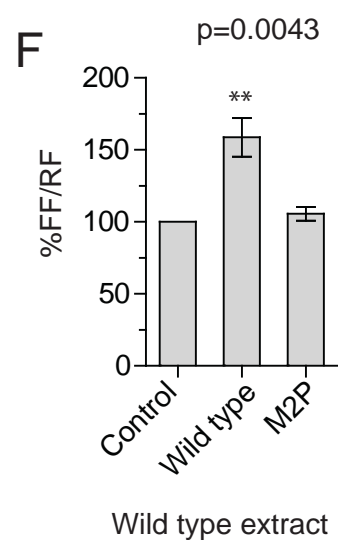
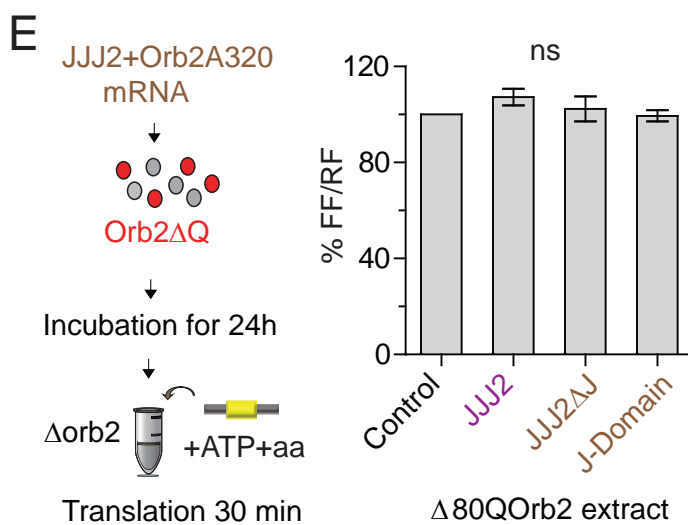
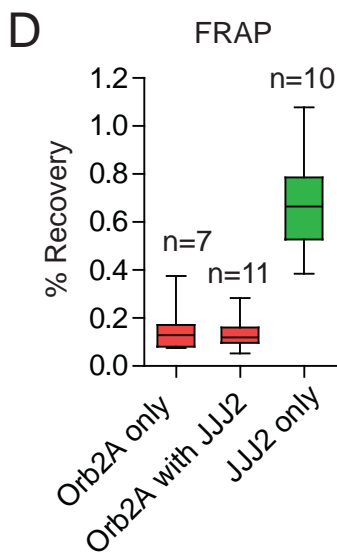
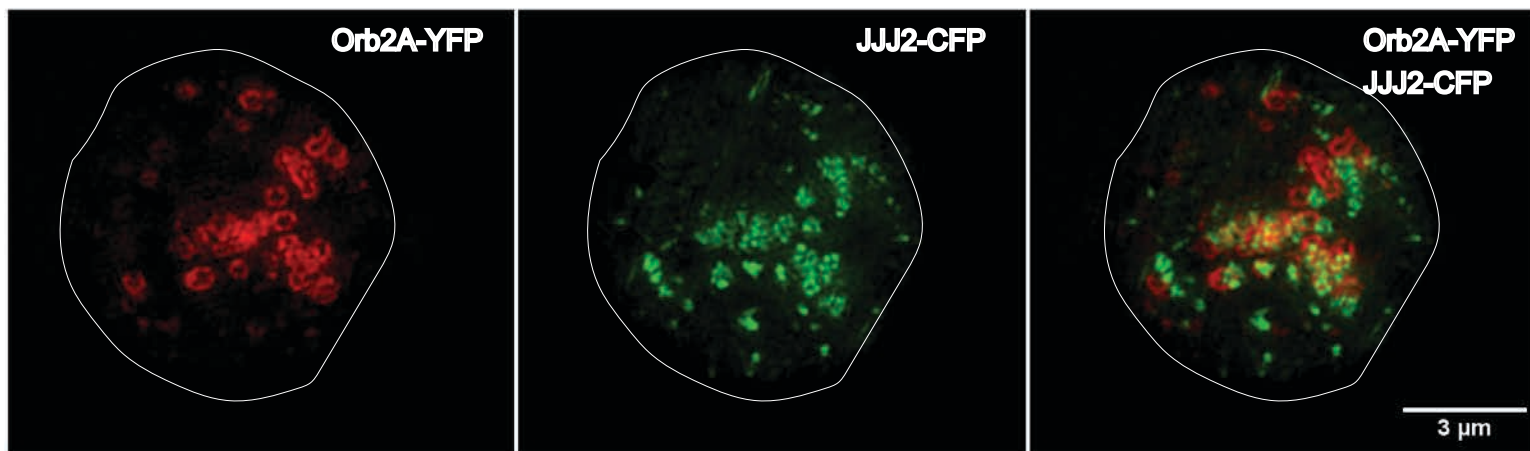


Figure S4

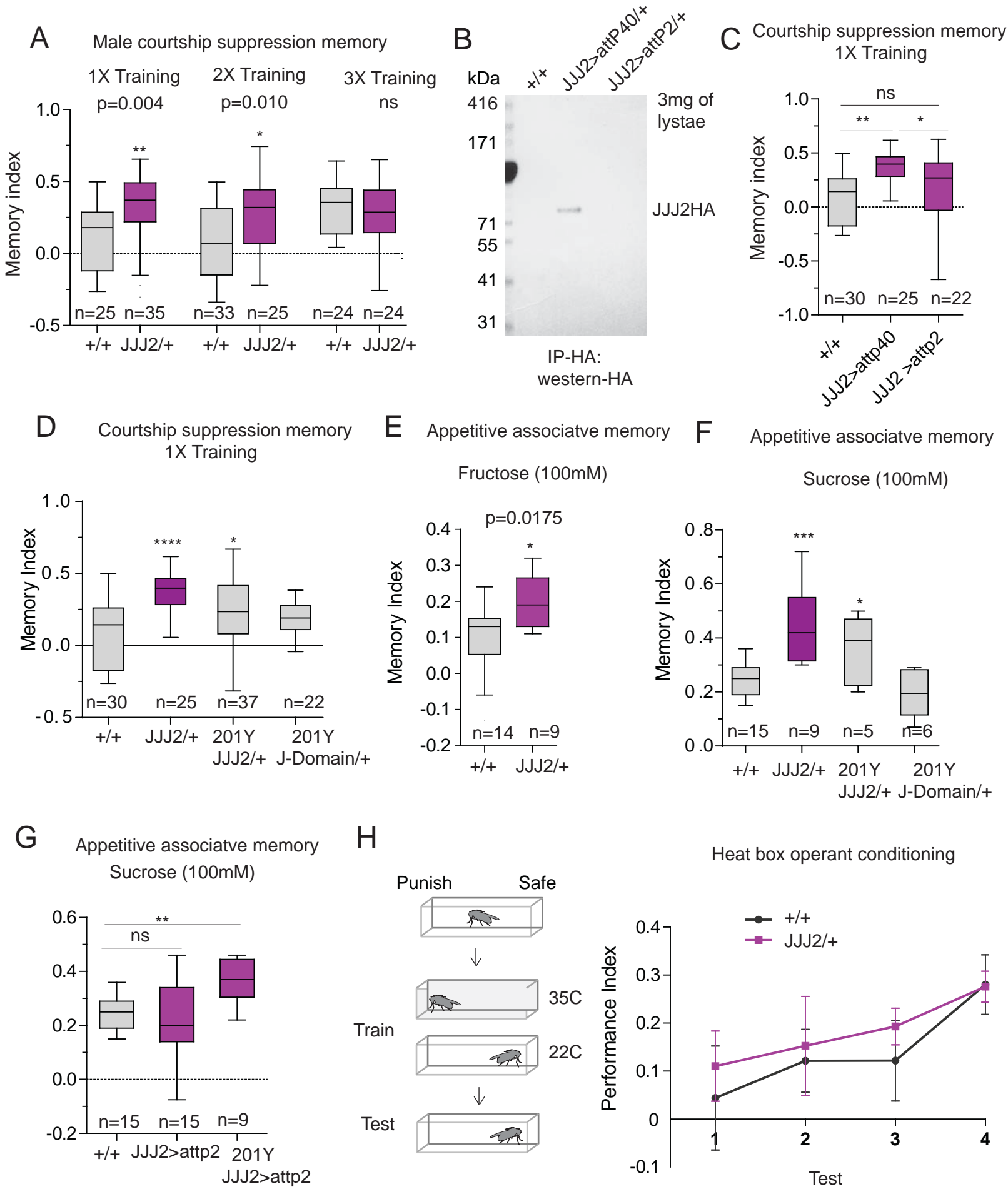


Figure S5

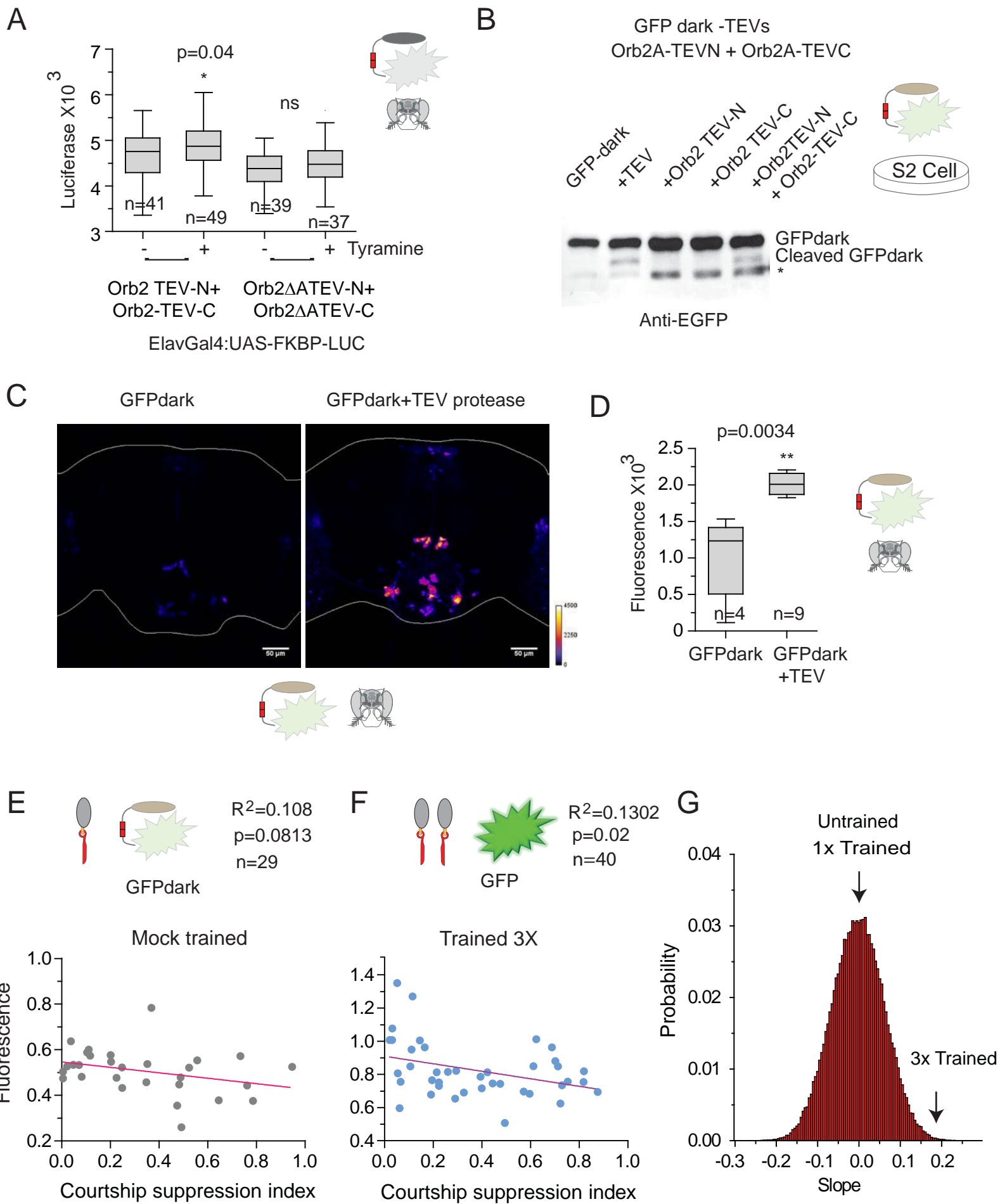


Figure S6

Supplemental Figure Legends:

Figure S1. Related to Figure 1, Figure 2 and Figure 3. A system to acutely and reversibly inactivate *Drosophila* Orb2 protein. (A) An S2 cell based screen of various tevS insertions in Orb2A protein that can be cleaved by TEV protease. The tevS was inserted in Orb2A protein at indicated positions. The modified Orb2A protein was expressed in S2 cell and total cell lysate was treated with 1ug of TEV protease overnight at 4 °C and analyzed in western. The bracket include cleaved C-terminal fragment of different sizes. The arrow points to N-terminal fragment of cleaved Orb2tevS(216). The faint band in wt, 23 and 88 is not an N-terminal fragment, they are immunoreactivity to *in vitro* added TEV protease. The * indicates an Orb2 immunoreactive band that likely represent an altered conformational state with slower electrophoretic mobility. (B) In male courtship suppression memory or (C) in appetitive associative memory paradigm flies with indicated genotype were fed with RU486 (blue) or vehicle (black) for 24h post-training. Only in flies expressing both modified Orb2 and TEV protease significant loss in memory was observed. (D) In male courtship suppression memory, extended feeding with RU486 (blue) from 24h before training and 24h after training resulted in memory loss even when Orb2 is restored (white bar) at 48h or 72h after training. Memory index for each group was plotted as mean \pm SEM and statistical significance was determined by unpaired t-test. *p < 0.05, **p < 0.01, ***p<0.001.

Figure S2. Related to Figure 4. Yeast chaperone deletion screen. (A) Schematic of the deletion screen: 1) Sup35 C-terminal was expressed under the Sup35 promoter from a Ura3-based plasmid in Sup35 deletion background; 2) The 38 non-essential chaperons were deleted in this background by homologous recombination using Kanamycin gene as a marker; 3) The Orb2AprD-Sup35C chimeric protein was expressed under the Sup35 promoter from a Leu2-plasmid; 4) Sup35P-Sup35C was then shuffled out using 5FOA resulting in Orb2AprD-Sup35C to be the only source of Sup35 in Hsp deletion background. (B) Representative examples of the effect of Hsp deletion in rich media (left) and -ade media (right). The Hsp40 family of chaperons are indicated in red, Hsp70 family in yellow, Hsp90 family in blue, CCT family in green and small Hsp family of chaperons in pink. (C) Unlike in wildtype strain where the [PRION]⁺ state is stably propagated, in JJJ2 deletion background Orb2AprD-Sup35C converts to [Prion]⁻ state with higher frequency. (D) JJJ2 deletion does not affect prion-like conversion of Orb2Bprd-Sup35C or the yeast prions RnqPrd-Sup35C and Mot3Prd-Sup35C fusion proteins.

Figure S3. Related to Figure 4. Yeast Hsp overexpression screen. (A) Schematic of the overexpression screen: 1) Sup35 C-terminal was expressed under Sup35 promoter from a Ura3-based plasmid in Sup35 deletion background; 2) Orb2AprD-Sup35C under Sup35 promoter was introduced and Sup35P-Sup35C was shuffled out using 5FOA; 3) 57 yeast chaperones under galactose inducible Gal1 promoter was introduced into this background; 4) The cells were grown in galactose media to induce expression of Hsps. (B) Representative examples of the effect of Hsp overexpression in rich media (left) and -ade media (right).

Figure S4. Related to Figure 4. JJJ2 interacts with Orb2 and enhances Orb2-dependent translation. (A) Schematic of the JJJ2 constructs used in various experiments. The JJJ2 Δ HPD lacks 6 aa HPD motif within the DNA-J domain, the JJJ2 Δ C1 lacks 14aa within the coiled-coil domain 1, JJJ2 Δ C2 lacks the 21aa within the coiled-coil domain 2, the JJJ2 Δ J lacks the first 66 aa encompassing the entire DNA-J domain and the J-only construct is comprised of just the first 66 amino acids. (B) Orb2A associates with JJJ2 in S2 cells. HA-tagged JJJ2 was co-transfected with untagged Orb2A. Orb2A was immunoprecipitated and probed for either JJJ2 or Orb2A. Deletion of conserved HPD-motif in DNA-J domain and deletion of coiled-coil domain 2 reduced but did not abolish interaction with Orb2A. It appears that only a small fraction of JJJ2 exists in a stable complex with Orb2A. (C) Super resolution images of JJJ2-CFP (green) and Orb2A-YFP (red) in a single S2 cell. Both forms punctate structure. Cell surface is marked with dashed line. (D) The nature of the Orb2A-aggregate is not altered by JJJ2. FRAP recovery of Orb2A puncta is similar in presence or absence of JJJ2. JJJ2 puncta itself is more dynamic than Orb2A puncta. (E) JJJ2 has no effect on translation of Orb2-dependent translation reporter in an extract that expresses a form of Orb2 that lacks the prion-like domain (Δ 80Q) or (F) translation in wild type extract of a reporter (M2P) that binds inefficiently to Orb2. Data is plotted as mean \pm SEM and statistical significance was determined by unpaired t-test or one way ANOVA. *p < 0.05, **p < 0.01, ***p<0.001.

Figure S5. Related to Figure 5. JJJ2 enhances long-term memory in *Drosophila*. (A) JJJ2-expressing flies forms better long-term memory after suboptimal training. Wild type (gray) and UAS-JJJ2-HA>attP40 (purple) flies were subjected to 1X, 2X or 3X male courtship suppression training sessions and memory was tested 24h after training. (B) Leaky expression of JJJ2HA protein in UAS-JJJ2>attP40 fly head. JJJ2HA was immunoprecipitated with anti-HA

beads from 3mg of fly head lysate of wild type, UAS-JJJ2>attP40 and UAS-JJJ2>attP2 flies and western blotted with anti-HA antibody. (C) Only in UAS-JJJ2>attP40 but not in UAS-JJJ2>attP2 flies significant increase in 24h courtship suppression memory was observed following 1X training. (D) Expression of JJJ2 (UAS-JJJ2>attP40) but not J-Domain in mushroom body neurons under 201YGal4 drivers enhances courtship suppression memory. Interestingly, although the memory was enhanced it was less compared to just UAS-JJJ2>attP40 flies suggesting more of JJJ2 is not necessarily conducive to better memory and integration of JJJ2 at attP40 site serendipitously provided the appropriate amount to aid memory formation. (E) JJJ2 enhances 24h memory when 100uM fructose was used as a weak stimuli in appetitive-associative memory. (F) Expression of JJJ2 but not J-Domain in mushroom body neurons under 201YGal4 drivers enhances appetitive-associative memory. (G) UAS-JJJ2>attP2 fly did not form better memory but when crossed to mushroom body 201YGal4 driver memory was enhanced. (H) Wild type and JJJ2 flies were trained in heat box operant conditioning. No difference in memory score between the groups was observed up to 4 trials. Memory was plotted as mean \pm SEM. One-way ANOVA was tested across groups, * $p < 0.05$, ** $p < 0.01$, *** $p < 0.001$, and **** $p < 0.0001$.

Figure S6. Related to Figure 6, Figure 7 and Table S1. Orb2 aggregation reconstitutes TEV protease activity and predicts memory strength. (A) Tyramine stimulation increase split-TEV protease activity. FKBP-DD-Luciferase was expressed pan-neuronally in Orb2-TEVN/Orb2-TEVC or Orb2 Δ A-TEVN/Orb2 Δ A-TEVC flies. Stimulation with 10 μ M tyramine significantly increased luciferase activity only in Orb2-TEVN/Orb2-TEVC flies. Unpaired t-test was used to compare the effect of tyramine. (B) GFP with a quenching peptide linked by a TEV protease recognition sequence (GFP-dark) was expressed in S2 cells. Co-expression of TEV protease or Orb2-TEVN/Orb2-TEVC resulted in cleavage of GFP-dark. We observed that only a small fraction of the GFP-dark is cleaved by the protease. The relative inefficiency worked in our favor because it reduced the noise in the system. Importantly the wildtype protease activity and the reconstituted protease activity were very similar for this substrate. The * indicates a nonspecific immunoreactive band. (C) TEV-protease enhances fluorescence from GFP-dark reporter. GFP-dark was expressed in adult fly neurons without or with TEV protease. For ease of comparison only a cross section of the fly brain is shown. (D) Quantification of fluorescence intensity of the same set of neurons from (C). Unpaired t-test was used to compare the effect of TEV. (E) Mock trained flies (ElavGal4::UAS-GFPdark; Orb2-TEVN/+), or (F) Unmodified GFP reporter that does not depend on TEV protease activity (ElavGal4::UAS-GFP; Orb2-TEVN/Orb2-TEVC) do not show positive correlation between courtship suppression and GFP intensity in the γ lobe. (G) Monte Carlo simulation of the memory index and fluorescence intensity of the data from Figure 7 and Table S1. Linear regression was used to analysis the correlation between courtship suppression index and GFP intensity. * $p < 0.05$, ** $p < 0.01$, *** $p < 0.001$, and **** $p < 0.0001$.

Supplemental Table 1-See excel file:

Table S1. Related to Figure 7 and Figure S6. The actual courtship suppression values and GFP intensity values of the mushroom body β and γ lobe. These values are used to generate the plots described in Figure 7 and S6. The table includes all positive and negative courtship values and only the positive values are used in the plots.

Supplemental Experimental Procedures:

Generation of transgenic constructs and fly strains.

Modified Orb2 genomic rescue construct: A 18,761 bp genomic fragment encompassing the Orb2 locus was cloned into a pattB vector to generate the pattB-Orb2 construct. The pattB-Orb2 construct was described in detail previously in Majumdar et al. [S1]. For this study the pattBOrb2 construct was further modified to generate the following constructs by counter selection BAC modification: 1) pattB-Orb2tevS216: the TEV protease recognition site ENLYFQG was inserted at the amino acid position 216 with respect to the Orb2A protein; 2) pattB-Orb2TEV-N: The N-terminal TEV fragment (1-118aa) was fused to the C-terminal of Orb2 with the linker sequence SRPGS; 3) pattB-Orb2TEV-C: The C-terminal TEV fragment (119-242aa) was fused to the C-terminal of Orb2 with the linker sequence SRPGS; 4) pattB-Orb2 Δ A-TEV-N and pattB-Orb2 Δ A-TEV-C: the first 8 amino acids specific to Orb2A protein, MYNKFVNF, were deleted from pattB-Orb2TEV-N and pattB-Orb2TEV-C constructs. All genomic rescue

constructs were inserted at attP2 site in the 3rd chromosome and then recombined with $\Delta orb2$. These constructs fully rescue the lethality of the Orb2 null mutant.

The pUAST-GFPdark construct: The quenching peptide [S2] with TEV protease recognition sequence (tevS-dark) 5'-actagtgagaatttgacttccaggaccatgtaacgactcaagcgaccactgtgtggcagcatcaattattggcattcttacttaattcttggactctggaccgtcttgactcgag-3' was synthesized with flanking SpeI and XhoI restriction sites. The EGFP fragment was amplified using primer pairs 5'-agaattcgatccatggtgagcaagggcgagg-3' and 5'-gactagtctgtacagctcgtccatgcc-3'. The PCR product was digested with EcoRI / SpeI and the pUAST vector was digested with EcoRI/ XhoI. The tevS-dark, EGFP and pUAST were ligated to make pUAST-GFPdark construct. The construct was injected using a standard P-element insertion method and multiple lines were generated. The line with the least background expression of GFP signal was used for this study.

The p10xUASTattB-3xHA-TEV construct: Full length TEV protease was first amplified with cccatgggagaaagctgtttaag and ctgagctagttcatgagttgagtcg primer pairs and then cloned into pENTER-D/TOPO vector. From TopoD vector the TEV protease then transferred into Gateway vector pTFHW (1123) to make N-terminal 3xHA tagged TEV protease. The 3xHA-TEV fragment was further amplified with agtcggtaccaacttaaaaaaaaaaa tcaaatgtaccatagatgtctctgac and agtctctagactagttcatgagttgagtcgcttcttaactgg and cloned into pJFRC81 vector (Addgene) to make p10XUASTattB-3xHA-TEV. The construct was then inserted at attP40 site in the 2nd chromosome.

pUASTattB-FKBPDD-Luciferase construct: The destabilized luciferase construct was made as described [S3] with following modifications. A fly optimized FKBP12L106P mutant variant was synthesized with TEV protease recognition sequence ENLYFQG at the c-terminal end. The fire fly luciferase gene was cloned in frame downstream of the TEV-protease recognition sequence.

pUASTattBJJ2construct. The yeast JJJ2 was cloned into TopoD donor vector (Invitrogen). Using LR-clonase (invitrogen) JJJ2 was transferred to pUAST-HAattB vector (kindly provided by Dr. Konard Basler). The pUAST constructs were inserted in the attP40 site in the 2nd chromosome or attP2 site in the 3rd chromosome.

Drosophila strains. The following *Drosophila* strains are used in this study: Elav-Gal4 (stock no.458), ElavRU-Gal4 (stock no.43642), 201Y-Gal4 (stock no.4400), 17d-Gal4 (stock no.51631), MzVum-Gal4 (stock no.29031), tubP-Gal80ts (stock no.7016), Cha-Gal80 (stock no.60321), Orb2RNAi (stock no.27050), UAS-GFP (stock no.1522), MB-Gal80 (stock no.64306), R11D09-Gal4 (stock no.48456). The stocks were obtained from the *Drosophila* stock center in Bloomington, Indiana.

RU486 feeding to induce TEV-protease expression. To induce expression of TEV protease using the GeneSwitchRU-Gal4 system we essentially followed the protocol described in McGuire et al. [S4] with some modifications. Briefly a 20mM stock solution of RU486 (Mifepristone, Sigma M8046) was prepared in 70% ethanol. The stock solution was diluted 1:20 in 2% sucrose (for courtship suppression memory) or distilled water (for olfactory appetitive conditioning) to a final concentration of 1mM. 70% ethanol diluted 1:20 in 2% sucrose solution (for courtship suppression memory) or distilled water (for olfactory appetitive conditioning) was used as vehicle control in feeding experiments. For olfactory appetitive conditioning, prior to training and testing flies were starved as groups in polystyrene vials (25 x 95 mm) containing Kimwipe soaked with 2.5mL 1mM RU486 for 18~22 hours. For male courtship suppression assay, flies were kept individually in polystyrene vials (25 x 95 mm) and before or after training exposed to a Kimwipe soaked with/without 2.5mL 1mM RU486 in 2% sucrose solution. In courtship conditioning to feed during training, 20mM stock solution of RU486 was diluted 1:40 in standard corn meal to a final concentration of 0.5mM. The flies were trained in 16 x 100 mm culture tubes (VWR) bottom of which were filled with the food. During no drug feeding period between training and testing, flies were kept in polystyrene vials containing standard corn meal. Where indicated, particularly in memory recovery experiments after training flies were kept in standard fly food for ≥ 2 hours before transferring to RU486 to ensure acquisition/encoding of memory.

Western Blot and Immunoprecipitation. For western blot analysis, fly heads were homogenized (2–4 μ l of buffer/head) in a PBS buffer containing 150 mM NaCl, 3 mM MgCl₂, 0.1 mM CaCl₂, 5% glycerol, 0.1% Triton X-100, 1% NP40, and protease inhibitors (Roche), and approximately 3–5 head equivalents of extract were used. For the immunoprecipitation to detect Orb2 oligomer, 1.5–2 mg of total protein was incubated with 1 μ g of the purified anti-Orb2 antibody 2233 (guinea pig) for 2 hr at 4°C and protein-A beads (Repligen) for an additional 2 hr. The IP then was blot with anti-Orb2 antibody 273 (rabbit).

Unlike monomeric Orb2, oligomeric/aggregated Orb2 is less abundant and the flies were fed 10uM tyramine to ensure detection of the aggregates. To quantify Orb2 oligomer/aggregates flies were fed 1mM RU486 + 10uM Tyramine in 2% sucrose solution or vehicle control+ 10uM Tyramine for 24h.

Yeast screening. For the yeast prion assay the nucleotide sequence of the n-terminal 160 amino acids of Orb2A were yeast optimized and fused in frame to Sup35 C-domain to create the chimeric construct Orb2Aprd-Sup35C. Using Gateway cloning strategy the chimeric construct was cloned into pAG414SUP35-ccdB-SUP35C (LEU, CEN plasmid, Sup35 promoter, SUP35C domain) Gateway vector (Invitrogen). The Orb2A-Sup35C (LEU selectable marker) construct was introduced into W303a Δ sup35 strain [MATa; leu2-3, 112; his3-11,-15; trp1-1; ura3-1; ade1-4; can1-100; SUP35::HygB; [*psi*-];[*PIN*+]] via plasmid shuffling. The yeast were grown in YPD media and plated on either YPD-agar or SC-agar lacking adenine and the [*PSI*+]] colonies were selected 2–3 days after plating. Selected colonies were grown in YP-glycerol plates to avoid petites. To determine frequency of prion-like conversion individual red or white colonies were grown in complete media and from a log phase culture 10X fold dilutions were plated in complete media and – Adenine plates. To determine heritability of prion or non-prion strains the colonies were streaked for multiple times. As we have reported previously [S5] the Orb2Aprd-Sup35C converts to the prion-like state in much higher frequency than Sup35. Therefore, in all cases we observed some growth in –Adenine plates, especially in higher cell count. For the overexpression screen cells grown in 2% Raffinose to mid log phase were transferred to 2% Galactose or 2% glucose containing media to OD⁶⁰⁰ ~0.4 and grown overnight before plating into appropriate media.

Generation of yeast Hsp-deletions in Sup35 deleted background. The *S. cerevisiae* W303a cells lacking the Sup35 gene was kindly provided by Dr. Susan Lindquist (MIT). In this strain the essential Sup35 function was provided by the C-terminal fragment of the Sup35 gene (Sup35C) from a URA-based plasmid. To knockout individual non-essential Hsps in this background we have used the yeast deletion library. In this collection each yeast open reading frame is replaced with a KanMAX module, which allows for selection of the deletion strain in geneticin plates. Briefly we isolated genomic DNA from the Hsp::KanMAX deletion strains and PCR-amplified the cassette with a ~100bp extension in both side for homologues recombination. The Δ sup35:Sup35P-Sup35C strains were transformed with the purified PCR fragments and the recombinants were selected in the geneticin plates. The deletion was verified by PCR using gene-specific and internal KanMAX primer pair followed by sequencing of the PCR product. Individual deletion strains were then transformed with Sup35P-Orb2Aprd-Sup35C plasmid with Leu-marker and via plasmid shuffling Sup35P-Sup35C was removed, resulting in Orb2Aprd-Sup35C being the only source of Sup35 protein. For overexpression, the Hsps were obtained from Yeast ORF collection in BG1805 vector or HIP FLEXGene ORF collection in BY011 vector. In both vectors the Hsps are cloned under the Galactose inducible yeast Gal1 or Gal10 promoter respectively.

In vitro translation assay with JJJ2. The *in vitro* translation assay was performed as described by Khan et.al [S6]. To perform *in vitro* seeding 5ng of Orb2A320 mRNAs or wild type or mutant JJJ2 mRNA were translated in WT or $\Delta orb2$ embryo extract for an hour at 26°C and then the reactions were incubated at 4°C for 24h. To test the effect of newly formed oligomer in translation, the Tequila translation reporters were pre-incubated for 30 mins with the oligomer and followed by translation in $\Delta orb2$ embryo extract for 30 mins.

The translation assay was carried out at 26°C in 25 μ L reaction volume, consisting of 50ng translation reporter, 40% (v/v) embryo extract, 16 mM Hepes-KOH, pH 7.4, 100 μ M amino acid mixture (Promega), 250 ng/ μ L *S. cerevisiae* tRNA (Roche Applied Science), 50 mM potassium acetate, 2.5 mM magnesium acetate, 100 μ M spermidine (Sigma), 20 mM creatine phosphate (Roche Applied Science), 80 ng/ μ L creatine kinase (Roche Applied Science), 800 μ M ATP, and 100 μ M GTP (Sigma). In all reactions 20U of RNase inhibitor (Invitrogen) was added prior to the addition of the translation reporter. Firefly and renilla luciferase activity was measured in 96-well plate reader (Perkin-Elmer 1420 Multilabel Counter) using the dual-glo luciferase assay system (Promega).

Single fly head luciferase assay. The flies were collected in a 1.5 ml Eppendorf tubes and snap-frozen in liquid nitrogen. The heads were separated from body by vortexing for 5-10 seconds and individual heads were transferred to the wells of 96-well flat-bottom micro-titer plate (Corning, NY, USA). The heads were then crushed using pipette tips in 50 μ L of PBS buffer containing 0.1% NP-40 (Sigma) and 0.1% Triton-X 100 (Sigma). 50 μ L of luciferase substrate (Promega) was added in each well, incubated for 10 minutes at room temperature and luciferase activity was measured using a luminometer.

Male courtship suppression assay. The male courtship conditioning assay was modified from that described previously [S7]. Each male virgin was isolated right after eclosion in standard food vials. When they mature to 4~5

days old, each virgin male was paired with a freshly mated female for one to three sessions of 2 h each, with a 30 min rest period in between. During training sessions flies were kept in 16 x 100 mm culture tubes (VWR) provided with standard corn syrup fly food. Memory performance was tested with a fresh-mated female at the indicated time point in a 1 cm diameter wheel. A courtship Index (CI) was measured as the fraction of time the tested male spent chasing the female in a 10 min interval using an automated ImageJ based program. The Memory Index or courtship suppression index (Fig 6) was calculated as: $\frac{CI_{Naive} - CI_{Trained}}{CI_{Naive}} \times 100$, where CI_{Naive} and $CI_{Trained}$ are the mean courtship indices for independent samples of naive and trained males, respectively.

Olfactory-Appetitive Conditioning. Flies were food deprived for 18 to 22 hour before conditioning in plastic vials containing kimwipes paper saturated with water. The wall of the training tube was covered with a Whatman filter paper saturated with 1M sucrose or indicated concentrations of sugar (Fig 5 & S5) and a second tube was prepared similarly except that the filter paper was soaked in just water. Starved flies were introduced into the elevator of a T maze and tested in groups of 50-70 flies. Flies were transferred to the tube containing sugar and exposed to an odor for 2 min. After 30 s of air stream, the flies were relocated in the elevator and shifted to the tube without sugar in the presence of the second odor for 2 min. For the 24hr test, flies were given standard cornmeal food for 3hr after training. They were then transferred to plastic vials containing a kimwipe soaked with water and starved for 17hr before testing. For the 48hr memory test, flies were given standard cornmeal food for 18–24hr after training and then were starved for 24–30 hr prior to testing. During the memory test, flies were introduced into the elevator and transported to a point where they have to choose between two air streams, one carrying the reward associated odor and the other with the non-associated odor. Animals were given 2 min to choose between the two odors. Different group of flies were trained in a reciprocal experiment in where the -reward/+reward odor combination were reversed (3-Octanol or 4-Methylcyclohexanol). The performance index (PI) is calculated as the number of flies in the reward odor minus the number of flies in the non-reward odor, divided by the total number of flies in the experiment. A single PI value is the average score of the first and the reciprocal experiment.

Image acquisition and quantification. To image the GFPdark signal, immediately after testing the flies were anesthetized and the brain was dissected into PBS. Images were acquired using a Zeiss LSM 510 Meta system in regular PMT imaging mode. The 488 laser was used to excite GFP through a HFT405/488/543 dichroic. Emission was reflected by a NFT 545 dichroic and through a BP 505-530 nm emission filter. A 20X, 0.8 NA plan apochromatic objective was used. Z-step size was 2.0 μ m. the pinhole was set to 53 μ m.

All analysis was performed in ImageJ. After background subtraction, each frame was spatially binned 2x2 and smoothed. To measure intensity in the α/α' , β/β' , and γ lobes, regions of interest (ROIs) were generated by hand over a representative, uniform region in the respective lobe, and average intensity was recorded. Z profiles over the respective region were analyzed to ensure the maximum intensity z-slice was used. GFP intensity in the γ lobe was normalized to the GFP intensity in the β/β' lobes to reduce the noise of variation in GFP-dark expression level. To eliminate potential bias in manual selection of ROIs, all data analysis was performed blindly on randomly named data sets: the analysis was done without the knowledge of 1) the genotype of the fly, 2) its memory score, and 3) what group the brain originated from, trained or untrained.

High resolution imaging to detect GFP-dark fibers was performed on a Zeiss LSM 780 confocal microscope equipped with an LD C-Apochromat 40x 1.1NA objective, a 40 μ m pinhole (1 Airy Unit), and a pixel size of 145 nm. Stacks were collected at a spacing of 700 nm and line averaging of 2. Excitation utilized a 488 nm laser with an MBS 488 dichroic. Detection was accomplished with the GaAsP spectral detector in integration mode and a gain of 788 in the wavelength range from 499 to 543 nm.

Structured Illumination Microscopy. Structured illumination microscopy was performed with an Applied Precision OMX Blaze microscope (Issaquah, WA, USA) equipped with PCO Edge sCMOS cameras and an Olympus 60x 1.42NA PlanApo N oil objective. Image stacks were acquired with 125 nm z resolution. CFP and YFP were excited with 440 and 514 nm excitation, respectively. SIM reconstruction and color alignment was accomplished using the Applied Precision software as reported previously [S8].

Number of trials (n) and Statistical analysis. All statistical analysis was performed using Graphpad Prism 6. All of the data met the assumption of homogeneity of variance, therefore unpaired two-tailed t-test or one-way analysis of variance (ANOVA) was performed, Tukey post-hoc test between pairs of samples. ANOVA tests for significance were performed at a probability value of 0.05 and more stringent values are listed in each figure where applicable. For

all experiments, each n is considered a biological replicate; separate trials used independent samples of genetically identical flies. In olfactory training experiments a single n is approximately 100-140 flies. Based on previous and ongoing experimental effect sizes, 8-10 double trials were generally judged to be adequate for memory experiments, unless effect sizes were strikingly large or variable. For courtship conditioning the n indicates number of individual male flies used in that group. In all long-term memory experiments, experimental manipulations for which a negative result was plausible or expected were always trained alongside a positive control.

For the correlation test between courtship suppression index and GFP intensity, flies with positive courtship suppression index were plotted and fit with linear regression, and the p -value and R^2 shown were also based on the population of positive courtship suppression index. Please see the supplemental table for the entire data set. In the mock trained and 1x trained group, flies either did not form any memory or had low memory. Therefore the number of flies with positive courtship suppression is ~50% of the total number of flies tested. In mock trained or 1X trained group the flies with high courtship suppression index represents random distribution of courtship activity,

Monte Carlo correlation analysis. In order to test the statistical reliability of the correlation between memory index and GFP-dark ratio, we performed a Monte Carlo analysis [S9]. Given that such analysis is strongly dependent on the shape of each variables statistical distribution, we chose a methodology which makes no assumptions for this shape. The method randomly shuffles the intensity ratio measurements and then assigns them to the unshuffled memory indices. This random shuffling was performed 100,000 times and each shuffle was fit with linear regression to create a probability distribution of slopes. The analyses were performed using custom written Java code available at <http://research.stowers.org/imagejplugins>. As expected, the distribution is centered at 0 and the probability was reported as the fraction of simulated slopes which were greater than or equal to the experimental value.

Supplemental References:

- S1. Majumdar, A., Cesario, W.C., White-Grindley, E., Jiang, H., Ren, F., Khan, M.R., Li, L., Choi, E.M., Kannan, K., Guo, F., et al. (2012). Critical role of amyloid-like oligomers of *Drosophila* Orb2 in the persistence of memory. *Cell* 148, 515-529.
- S2. Nicholls, S.B., Chu, J., Abbruzzese, G., Tremblay, K.D., and Hardy, J.A. (2011). Mechanism of a genetically encoded dark-to-bright reporter for caspase activity. *The Journal of Biological Chemistry* 286, 24977-24986.
- S3. Sellmyer, M.A., Thorne, S.H., Banaszynski, L.A., Contag, C.H., and Wandless, T.J. (2009). A general method for conditional regulation of protein stability in living animals. *Cold Spring Harbor protocols* 2009, pdb prot5173.
- S4. McGuire, S.E., Mao, Z., and Davis, R.L. (2004). Spatiotemporal gene expression targeting with the TARGET and gene-switch systems in *Drosophila*. *Sci STKE* 12.
- S5. Hervas, R., Li, L., Majumdar, A., Fernandez-Ramirez Mdel, C., Unruh, J.R., Slaughter, B.D., Galera-Prat, A., Santana, E., Suzuki, M., Nagai, Y., et al. (2016). Molecular Basis of Orb2 Amyloidogenesis and Blockade of Memory Consolidation. *PLoS biology* 14, e1002361.
- S6. Khan, M.R., Li, L., Perez-Sanchez, C., Saraf, A., Florens, L., Slaughter, B.D., Unruh, J.R., and Si, K. (2015). Amyloidogenic Oligomerization Transforms *Drosophila* Orb2 from a Translation Repressor to an Activator. *Cell* 163, 1468-1483.
- S7. McBride, S.M., Giuliani, G., Choi, C., Krause, P., Correale, D., Watson, K., Baker, G., and Siwicki, K.K. (1999). Mushroom body ablation impairs short-term memory and long-term memory of courtship conditioning in *Drosophila melanogaster*. *Neuron* 24, 967-977.
- S8. Zhou, C., Slaughter, B.D., Unruh, J.R., Guo, F., Yu, Z., Mickey, K., Narkar, A., Ross, R.T., McClain, M., and Li, R. (2014). Organelle-based aggregation and retention of damaged proteins in asymmetrically dividing cells. *Cell* 159, 530-542.
- S9. Bevington, P.a.D.K.R. (2003). "Data Reduction and Error Analysis for the Physical Sciences." McGraw-Hill, 194-218.